General Disclaimer

One or more of the Following Statements may affect this Document

- This document has been reproduced from the best copy furnished by the organizational source. It is being released in the interest of making available as much information as possible.

- This document may contain data, which exceeds the sheet parameters. It was furnished in this condition by the organizational source and is the best copy available.

- This document may contain tone-on-tone or color graphs, charts and/or pictures, which have been reproduced in black and white.

- This document is paginated as submitted by the original source.

- Portions of this document are not fully legible due to the historical nature of some of the material. However, it is the best reproduction available from the original submission.

NASA CR- 159925

ELECTROSTATICALLY FOCUSED INTENSIFIED CHARGE COUPLED DEVICES

James W. Walker

Texas Instruments Incorporated

Dallas, Texas 75222

August 1977

Final Technical Report for Period 8 July 1976 - 8 July 1977

Prepared for

GODDARD SPACE FLIGHT CENTER

Greenbelt, Maryland 20771

TABLE OF CONTENTS

LIST OF TABLES

LIST OF ILLUSTRATIONS

TABLE OF CONTENTS
(continued)

SECTION I

INTRODUCTION

This report presents the work performed by Texas Instruments under NASA/ Goddard Space Flight Center Contract No. NAS5-23578 to develop intensified charge coupled devices (ICCDs) for photon-counting applications. This contract called for the fabrication, characterization, and delivery of four electrostatically focused intensified CCDs (EFICCDs) and for a study of ways to diminish CCD degradation during tube processing.

An ICCD consists of a charge coupled imager, mounted on a suitable header, incorporated in a vacuum bottle with a photocathode and provision for accelerating and focusing the photoelectrons onto the CCD. The CCD imagers employed in this contract were 100 x 160 arrays featuring 22.9 μm (0.9 mil) x 22.9 μm (0.9 mil) pixels, buried channel, and three-phase clocking using two-level aluminum metallization. Figure 1 is a photograph of this bar. For electron input (EBS mode), the devices must be backside-illuminated to eliminate charging effects in the frontside oxide layers. In addition, the device must be thinned to minimize diffusion degradation of MTF. Finally, due to the recombination of electrons at the silicon surface, the backside must have an excess or accumulation of the dopant boron atoms to create an electric field that will force electrons away from this surface.[1] Thinned CCD arrays are shown in Figure 2.

These arrays must be mounted on headers that are compatible with vacuum tube technology and that allow lead bonding on the frontside and illumination at the backside. Figure 3 shows the design of the header employed during this program. After alloying and bonding the device to the header, an inner cap is welded to the seal flange to provide vacuum capability. The header is then welded to the tube body at the edge of the tube flange.

The ICCDs fabricated under this contract were fabricated by Varo Electron Devices, Inc. This was accomplished by replacing the output phosphor on the

1
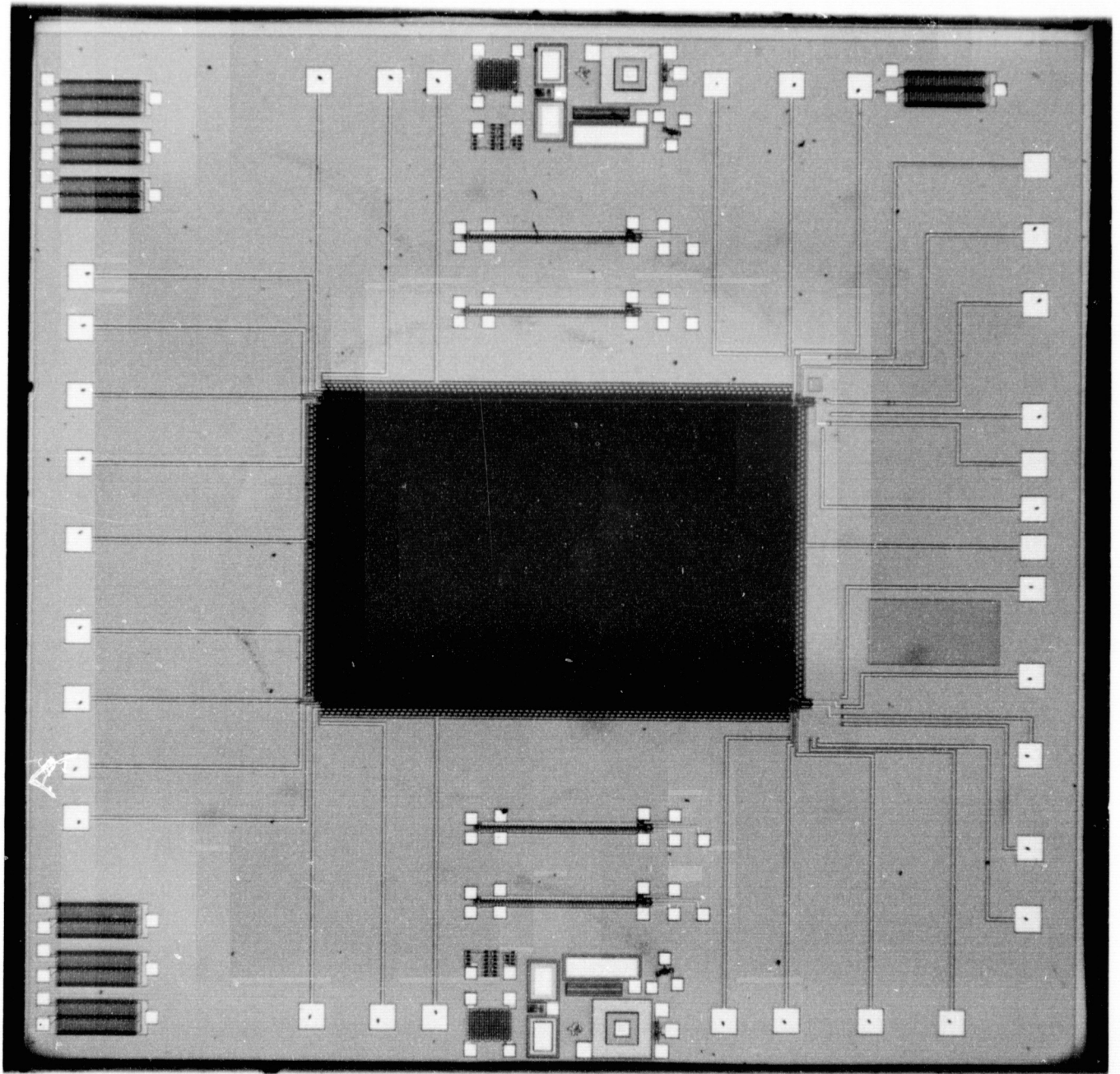
Figure 1   100 x 160 Element Imager
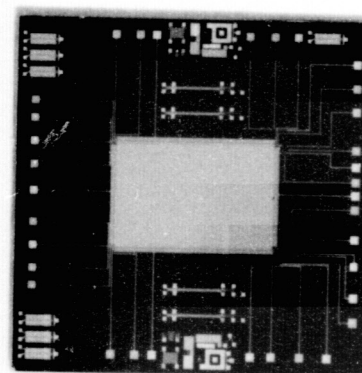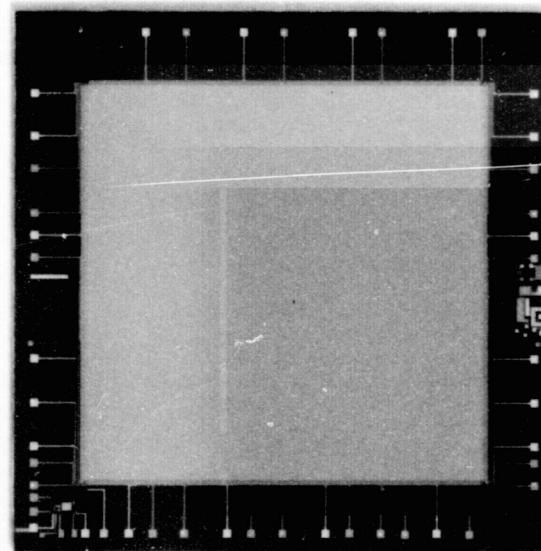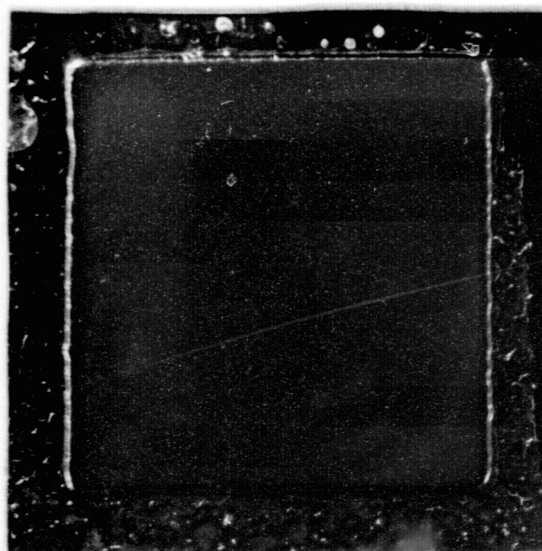
Figure 2   Thinned CCD Arrays
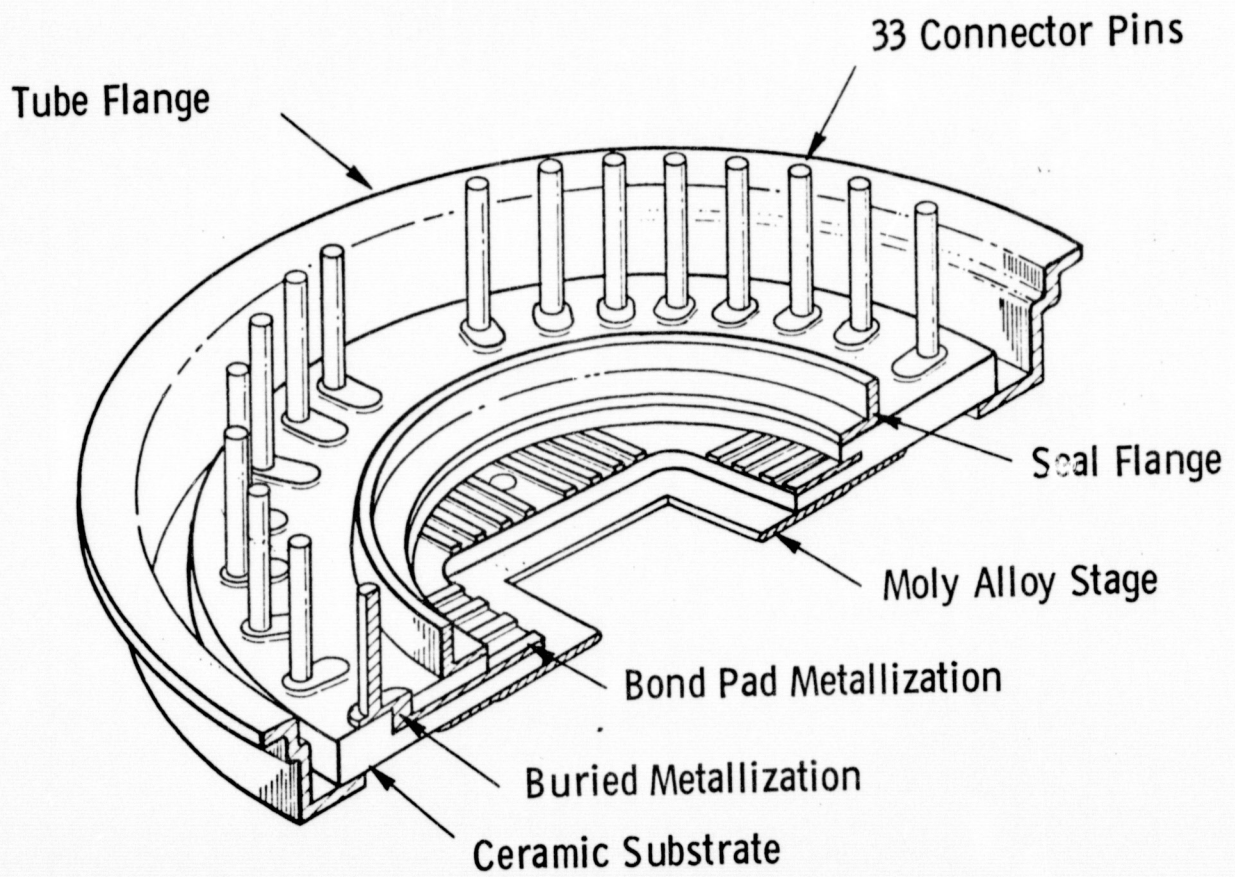
Figure 3 Cutaway Drawing of Tube Header

4

Varo Model 2561 electrostatically focused image intensifier with the CCD header. Figure 4 shows a completed ICCD together with front and back views of the header employed. After completion of the processing, the tubes were potted, with three leads provided for accelerating and focus voltages.

Under this contract, four ICCDs were fabricated. The characteristics of these devices before and after tube processing are presented in Section III of this report.

Early work on ICCDs had indicated a potential problem caused by degradation of bond strength during the high temperatures encountered during tube processing. Under this contract a study was made to quantify this effect and to develop a method of preventing this degradation. Results of this bond pad protection development are presented in Section II, together with the results of a study of the accumulation process that has led to reproducible spectral response characteristics. Conclusions are given in Section IV.
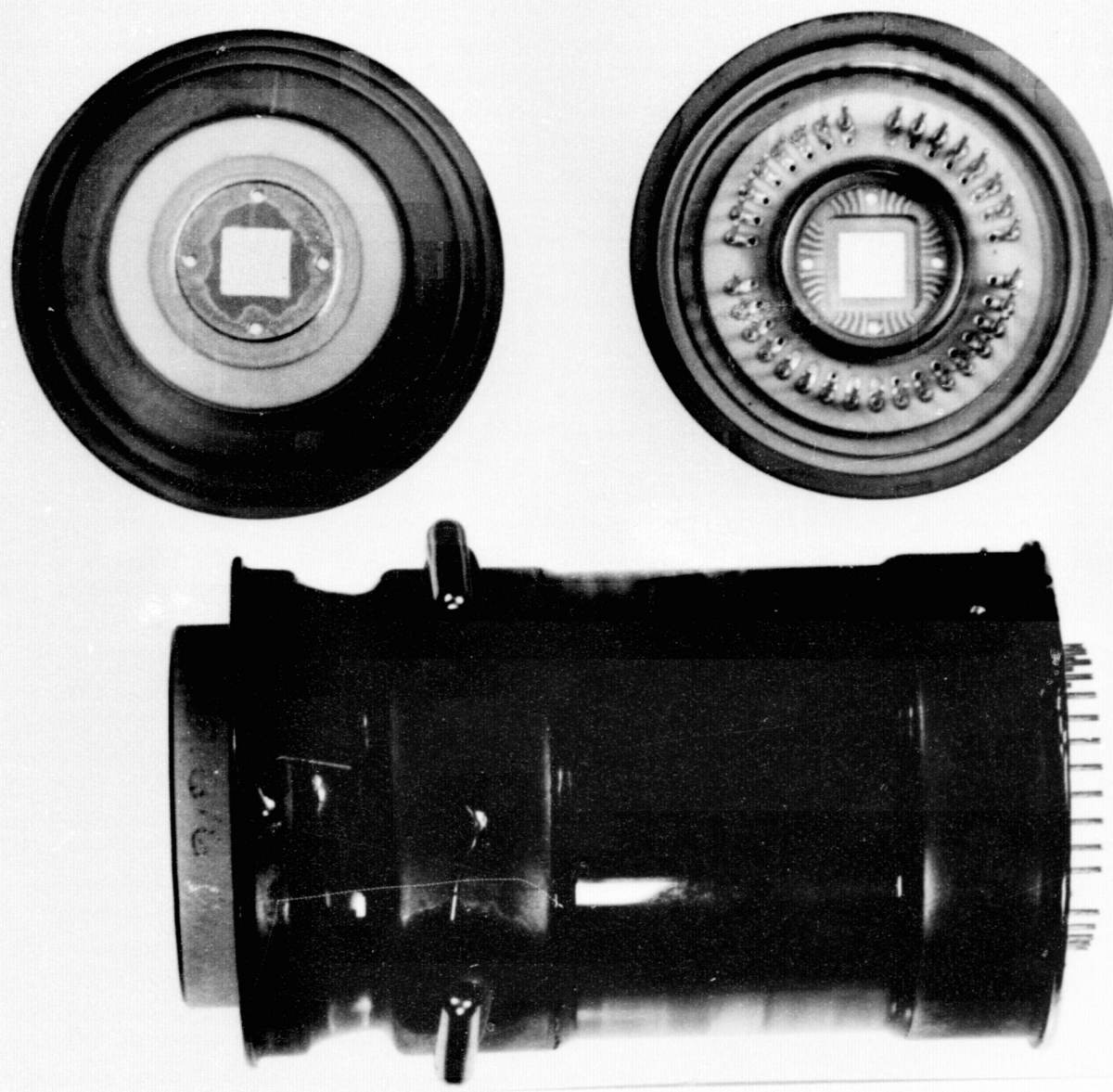
Figure 4 25 mm Electrostatically Focused, Intensified Charge Coupled Device

SECTION II
PROCESS DEVELOPMENT

A. Bond Pad Protection

1. Bond Strength Degradation

Electrical interconnection is made between the array and the header using gold wire, thermocompression-bonded between the aluminum metallization of the array and the gold metallization of the header. In early work on ICCDs, it was observed that occasionally the gold metallization would separate from the aluminum bond pad after the high temperature (350°C) bake associated with tube processing. This problem was found to be caused by intermetallic formation which led to the introduction of voids in the aluminum-to-gold interface. This effect has been discussed by Philofsky.[2] According to Philofsky, during the anneal of aluminum-to-gold couples, intermetallic compounds are formed. (Some of these are purple, which leads to the term "purple-plague.") To form these compounds, diffusion of the two metals occurs. In the case of aluminum bond pad, it is possible for enough aluminum to be absorbed by the gold wire to weaken the contact to the array. This can result in bond failure.

Experiments were performed to quantify this effect for typical bonds undergoing a 350°C anneal. To do this, bonding samples were prepared by evaporating the standard thickness of aluminum bond pads (11,000 Å) onto oxidized silicon slices and patterning the metal using the second-level metal mask of the 100 x 160 bar. Gold wire was then thermocompression-bonded from one bond pad to a neighboring pad to form loops of wire. Ten to twenty loops per slice were prepared. Bond strength was determined by pulling on these loops with a calibrated force, increasing this force until either the wire broke or the bond failed. The minimum acceptable pull strength for a bond is generally accepted to be 2 dynes. Measurements on unannealed samples indicated pull strengths ranging from 6 to 14 dynes, all breaks occurring in the wire.

The initial experiment consisted of isothermal anneals at 350°C. Figure 5 presents the results of the measurements of pull strength after anneals of two, four, six, and eight hours. Open circles represent wire breaks, Δ's represent bond failure, and dark circles represent the numeric average. The data indicate the following:

(1) There is a gradual degradation in bond pull strength with increasing anneal time; initially, all failures are wire breaks, and finally, all failures are bond separation;

(2) Pull strength degradation seems to saturate with increasing anneal time;

(3) Considerable scatter exists in the data; and

(4) Only one value falls below the 2 dyne limit.

Typical annealing results are illustrated in Figure 6. Figure 6(a) shows a bond prior to anneal. Figure 6(b) shows this same bond after anneal. The dark area surrounding the bond is the intermetallic formation. Figure 6(c) shows a bond pad after pull tests that resulted in bond separation. In the center of the bond area, the aluminum has been completely absorbed, revealing the underlying oxide.

In an attempt to determine causes of the scatter in the data, anneal tests were performed on bonds with varying bond diameters. Small bonds (about twice the wire diameter of 1 mil), medium bonds (about three times the diameter), and large bonds (about four times the diameter) were prepared. The results of the pull tests after anneal were significant. All the small bonds annealed failed the 2 dyne limit, all the large bonds passed the 2 dyne limit, and the medium bonds resulted in a mixture of passes and failures. All bonds displayed visual degradation similar to Figure 6(b).
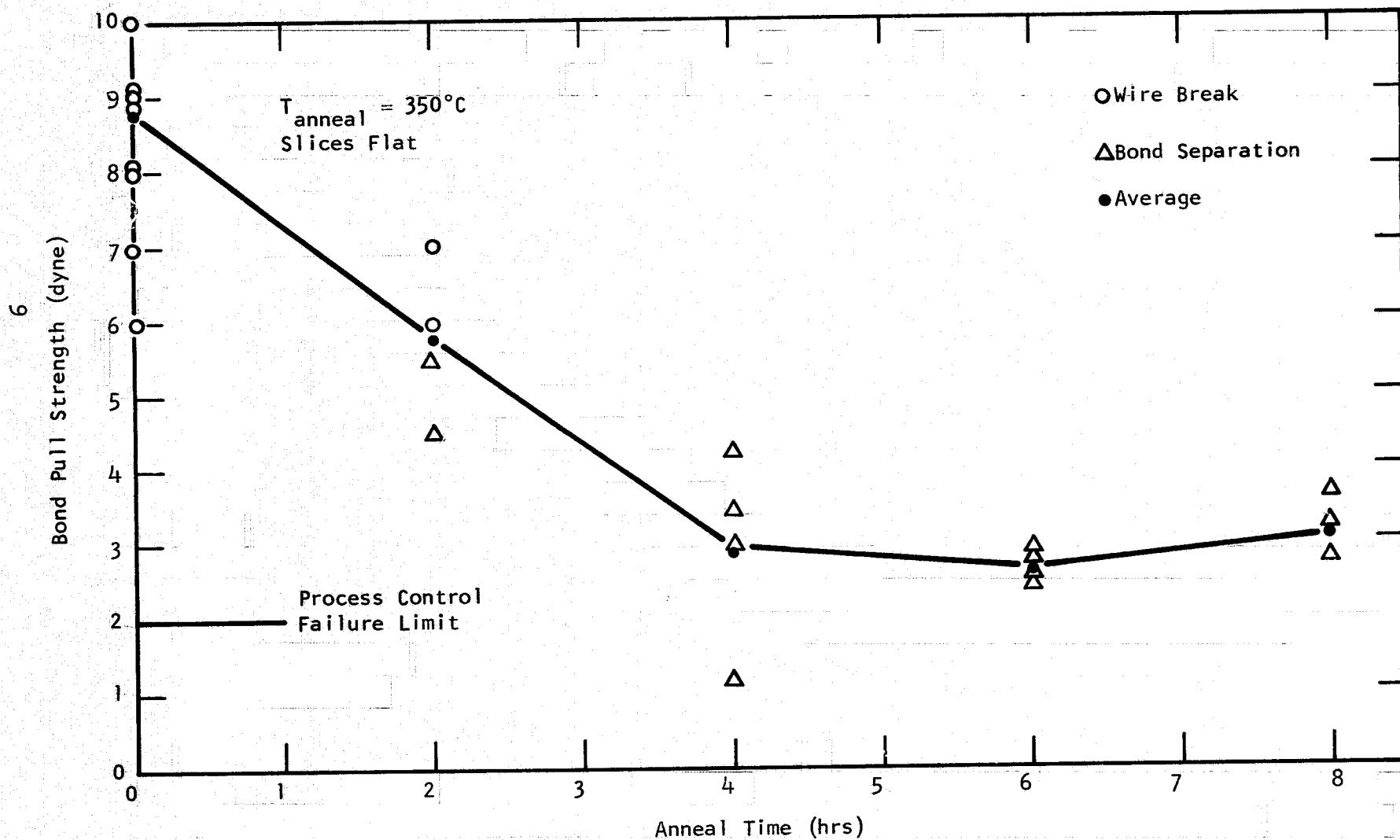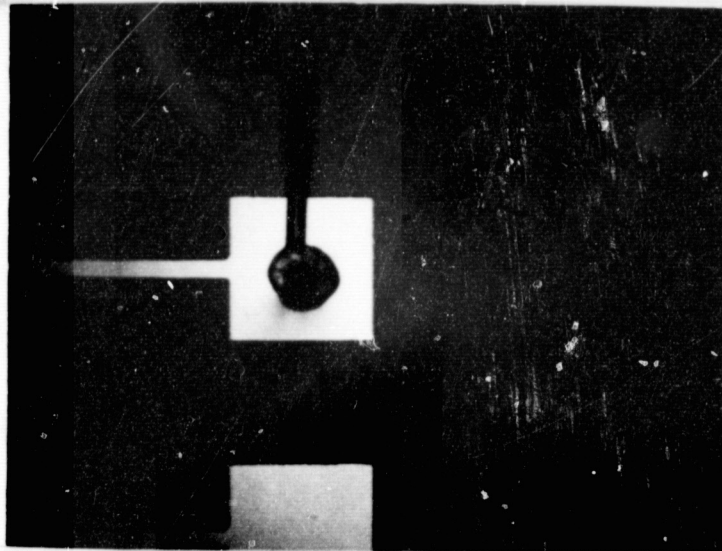
Figure 5   Bond Strength Degradation at 350°C
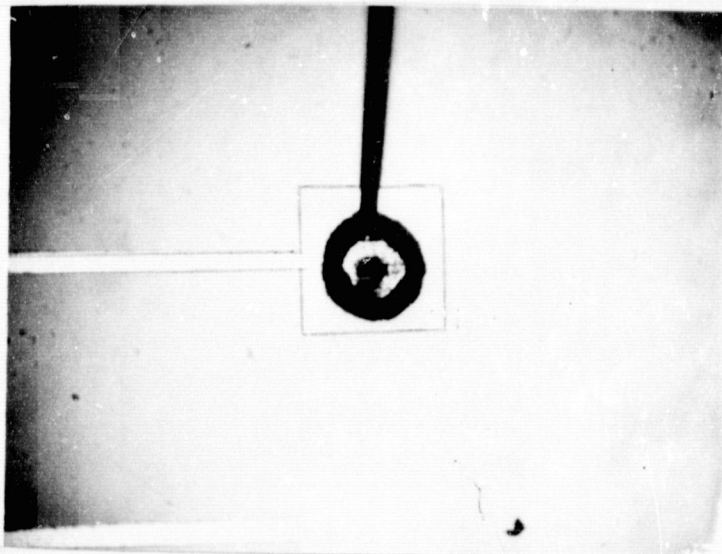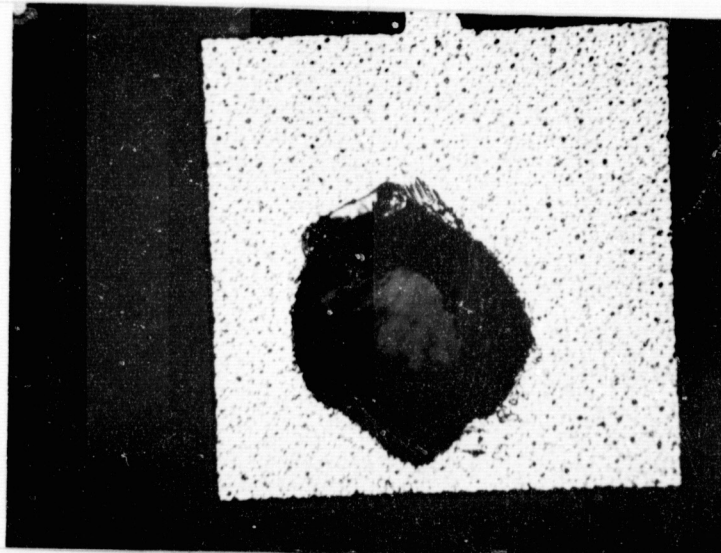
Figure 6 (a) Bond Appearance Before Anneal. (b) Bond Appearance After Anneal.
(c) Bond Pad Appearance After Bond Separation.

This result seems to indicate that the pull strength after 350°C anneal is related to the periphery of the gold-aluminum contact area. Since the pull strength degradation is due to the depletion of aluminum, this result can be understood by observing that the supply of aluminum for diffusion parallel to the oxide surface is not limited compared to the aluminum for diffusion perpendicular to the surface. This means that as annealing continues, the aluminum under the central area of the bond is depleted by diffusion into the gold wire, whereas around the edges of the bond, aluminum is replenished by diffusion from the unbonded pad area. In the final state, the bond is attached only around the periphery, and bond strength should be directly proportional to the bond circumference.

Assuming this analysis to be correct, the previously observed bond failures were caused by bonds with circumferences somewhat smaller than the normal. After these results were obtained, bonding procedures were changed to insure that all bonds were made with circumferences large enough to insure bond reliability.

2. Bond Pad Protection Process

In addition to efforts to determine the cause of bond failure and to quantify the effect, the contract also provided for the development of a process to eliminate bond strength degradation. Since the cause of this degradation is the formation of compounds of aluminum and gold, such a process must provide for bonds which provide separation of these two elements. Elimination of one of the elements would be difficult. Aluminum is an integral part of the processing of CCD arrays, and its elimination would require extensive process development, beyond the scope of this contract. Gold is required on the headers for low contact resistance and for lifetime and reliability considerations. Therefore, a process was required which would allow separation of the aluminum bond pads from the gold of the bond wire and header.

11

Aluminum wire was not considered because it required ultrasonic bonding techniques, which could cause membrane fracture. Similar problems would be expected at the bond of the aluminum wire to the gold header.

The process selected for development called for the insertion of a barrier metal (such as molybdenum, chrome, or titanium) between the aluminum and the gold. This could be done by depositing the barrier metal over the aluminum and patterning both metals at once. However, these metals are generally too hard to allow thermocompression bonding. For this reason, gold must be deposited over the barrier metal to allow bonding. An additional problem is that the barrier metals are deposited in thin layers (1000 $\overset{\circ}{A}$) to avoid cracking. The possibility exists for the thermocompression bond to penetrate this thin barrier metal during bonding. For this reason, the bonding area must be offset from the original aluminum bond pad.

This requirement for offset bond pads presents the final problem. Since the aluminum is 11,000 $\overset{\circ}{A}$ thick, a step coverage problem exists when the 1000 $\overset{\circ}{A}$ barrier metal is deposited. It would be expected that the metal on top of the pads would be separated from the remainder of the offset pad and electrical continuity would not exist. For this reason, it is necessary to introduce a beveled edge to the aluminum bond pad. A process is used which allows continuous metal films to be produced from the top of the aluminum bond pad to the surrounding oxide. Figure 7 shows the results of the application of this process to an aluminum bond pad.

The steps in the bond pad protection process are illustrated in Figure 8. Figure 8(a) shows an aluminum bond pad after completion of standard processing. The area of the bond pad is reduced and its edges are sloped as shown in Figure 8(b). The slice is then ready for deposition of the barrier metal and the gold. These two layers are patterned to form an offset bond structure as shown in Figure 8(c). Thermocompression bonding is performed on
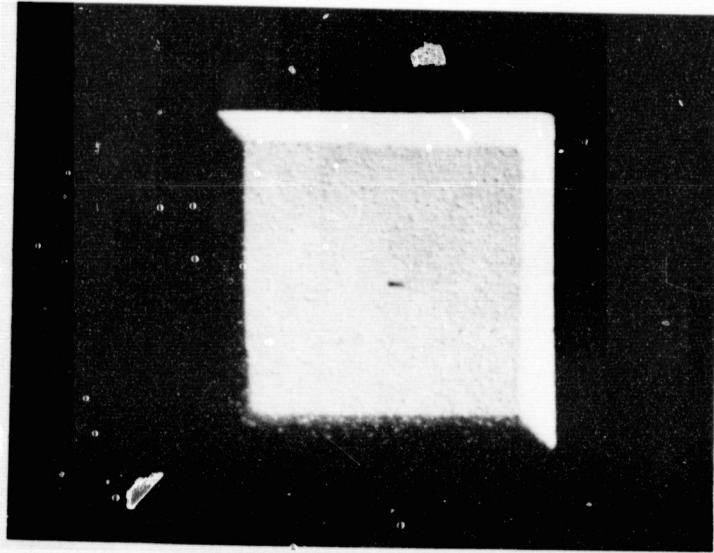
Figure 7   Aluminum Bond Pad with Sloped Edges
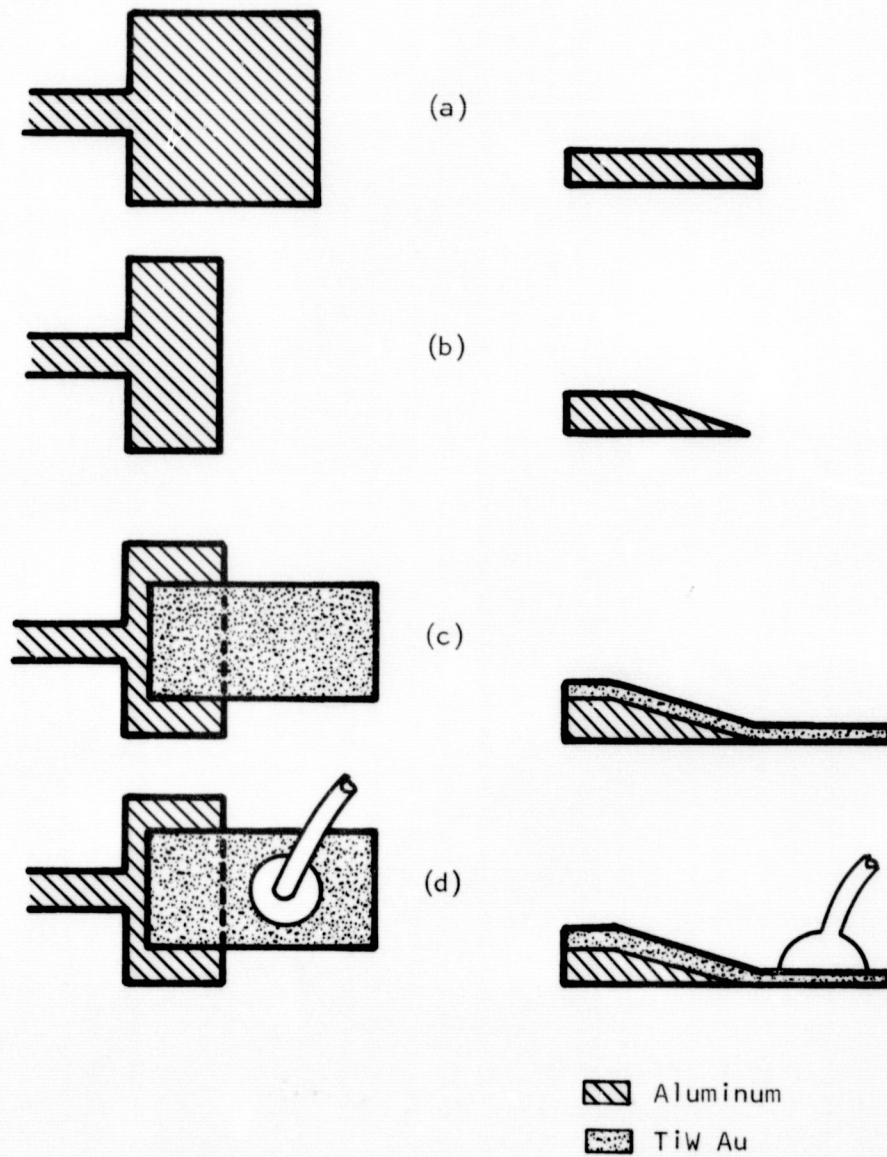
Figure 8 Bond Pad Protection Processing Steps

14

the offset area of the pad as shown in Figure 8(d). This process was successfully implemented on CCD arrays as indicated in Figure 9. Tests were performed to determine if any electrical continuity problems existed. In no case was an electrical open observed between the offset bond area and the aluminum metallization.

Other potential problems involved with this process were investigated. One possibility is the introduction of metal shorts during the patterning process, and another is an increase in dark current caused by the metal deposition processing. Careful measurements of device yield before and after bond pad protection processing indicated no loss of functional devices due to this processing. Dark current changes were monitored using test diodes. Measurements of the dark current before and after processing indicated an average increase in dark current of 10% of the initial value. This was considered to be acceptable, and no attempt was made to eliminate this increase.

Anneal tests were performed to verify that these new bond pads would eliminate bond degradation during tube processing. Samples of the offset pad structure were prepared and bond loops constructed as shown in Figure 10. Three barrier metals were tested: chrome, molybdenum, and a mixture of titanium and tungsten. Pull tests were performed after anneals at various times and temperature. Control samples of unprotected aluminum bond pads with uncontrolled bond size were also annealed. Typical results for the case of titanium-tungsten are given in Table 1. Similar results were obtained for the case of molybdenum and chrome.

As this table indicates, the protected bond pads exhibited no bond strength degradation introduced by annealing. In no case, for any of three barrier metals considered, did a bond separate; all failures occurred in the wire at pull force well above 2 dynes.

15
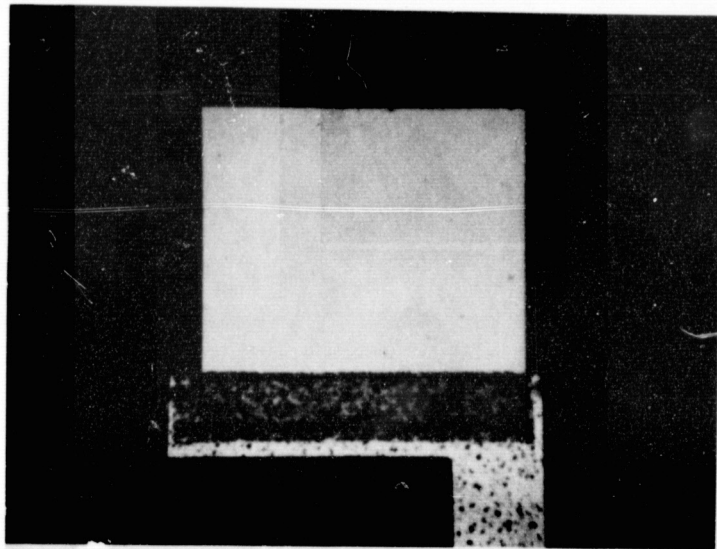
Figure 9 Bond Pad Protection Structure
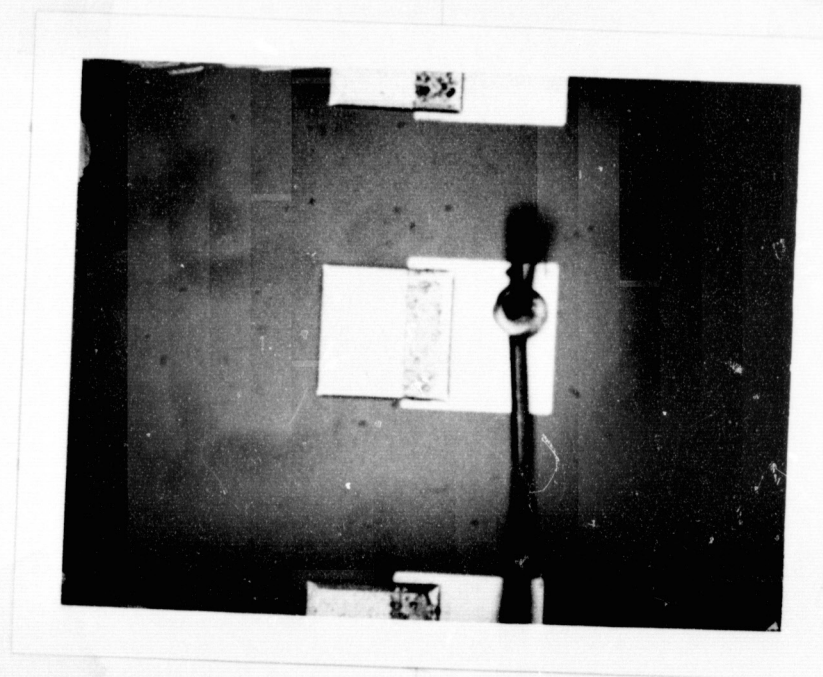
Figure 10 Offset Bond Pad Structure for Anneal Tests

Table 1

Anneal Test Results for Titanium-Tungsten-Protected Bond Pads

Anneal Temperature(°C)	Time(hrs)	Unprotected Pads		Protected Pads	
		Pull Strength(dynes)	Failure Mode	Pull Strength(dynes)	Failure Mode
300	3	7.0	wire	7.5	wire
		5.0	wire	7.0	wire
		6.5	wire	7.0	wire
	6	9.0	bond	7.0	wire
		3.0	wire	6.0	wire
		6.0	wire	8.0	wire
	8.5	7.0	bond	7.5	wire
		0.5	bond	7.0	wire
		8.0	wire	7.0	wire
350	3	7.0	wire	9.0	wire
		5.0	bond	6.5	wire
		9.5	bond	8.0	wire
	6	9.0	wire	6.0	wire
		7.0	bond	7.0	wire
		5.0	bond	9.0	wire
	10	0.0	bond	7.0	wire
		2.0	bond	7.0	wire
		7.0	wire	7.0	wire
400	4	2.0	bond	6.5	wire
		3.5	bond	6.5	wire
		9.0	wire	7.0	wire
	6	0.5	bond	6.0	wire
		3.0	bond	7.0	wire
		5.0	bond	8.0	wire
	9	1.0	bond	7.0	wire
		2.0	bond	7.0	wire
		7.0	wire	7.5	wire
450	3	6.0	bond	8.0	wire
		6.0	wire	7.0	wire
		8.0	wire	9.0	wire
	6	7.0	bond	9.0	wire
		6.0	bond	7.0	wire
		6.5	wire	7.5	wire
	9	7.0	wire	8.0	wire
		8.0	bond	6.0	wire
		6.0	bond	7.0	wire

18

At higher temperatures, some intermetallic formation was observed. Figure 11 shows a bond annealed at 450°C for nine hours. In this figure the area of overlap of the aluminum and the gold bond pads is purple. Even in cases like this, failure was observed to occur in the wire rather than at the bond.

These tests indicated that all three barrier metals are acceptable. Titanium-tungsten was chosen for the remaining work since it is employed somewhat more often in semiconductor devices.

At this point in the development, all evaluation had been performed using test structures. The remaining step was to process a functional device through the bond pad protection steps and then through the tube fabrication steps. The first time this was done, the device failed to operate after the 350°C tube bake due to the introduction of metal shorts in the parallel section. Optical inspection of the device revealed discolored regions in the parallel section. Other functional devices with protected bond pads were annealed at 350°C with similar results.

The cause of this problem was traced to the nitride overcoat. Bond pad protection processing for these devices had begun after the nitride had been deposited and patterned. The titanium-tungsten and gold were therefore deposited over the nitride. It was postulated that for some reason related to the nitride, patches of these metals remained after patterning the bond pads. These patches would be isolated from the parallel section metal by the nitride and therefore would not be electrically observable. However, during the anneal, these metals apparently diffused through the nitride, resulting in the observed discolored regions and in electrical shorts in the parallel section. This analysis was verified by taking functional chips, stripping the nitride overcoat (and thereby the residual metal), and annealing. No failures were observed with these chips, and successful tube processing resulted.
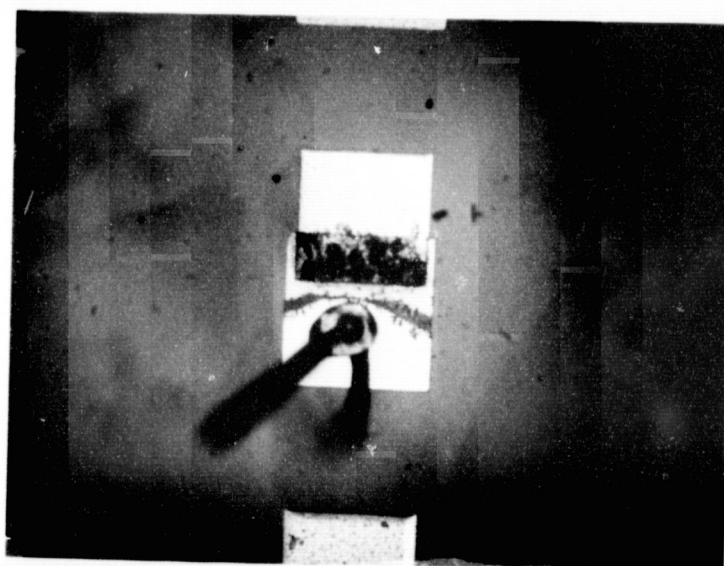
Figure 11   Intermetallic Formation at 450°C

The problem was eliminated from existing chips by stripping the nitride. In future processing, the nitride overcoat will be applied after the bond pad protection process has been completed. The last two devices delivered under this contract had protected bond pads.

3. Conclusions

At the beginning of this contract, there was serious concern about the reliability of the bonding scheme for ICCDs. As a result of the work described here, two solutions have been obtained. One results from the observation that, despite some degradation, bond strength can be conserved in the aluminum-gold system by using bonds with sufficiently large circumferences. This procedure was implemented during the development of the bond pad protection process. Approximately 30 ICCDs have since been fabricated using these bonds, with no indication of bond failure. The second solution completely eliminates bond degradation by inserting a barrier metal between the gold and aluminum. ICCDs have been fabricated with protected bond pads with no significant change in the CCD characteristics.

In view of the equal success of these two solutions, it is recommended that the standard ICCD processing continue to be the gold-aluminum system due to the increased processing time and cost associated with the barrier metal process. However, the development of this barrier metal process could have great significance in the future development of backside-illuminated CCD imagers. It is a relatively simple matter to take the process as it now exists and extend it to allow the plating of gold on the bond pads to sufficient thickness for the construction of beam leads. Beam leads would allow the bonding of devices frontside down, greatly simplifying the header design required. In addition, beam leads could provide a method of relieving the strain currently introduced by the different thermal expansion coefficients of the silicon and the molybdenum alloy stage (see Figure 3).

B. Characterization of the Accumulation Process[*]

1. Characterization Requirements

As discussed in the introduction, the thinned surface of a backside-illuminated imager must have an accumulation layer of boron atoms to minimize signal loss at this surface. This can usually be accomplished by diffusion of boron atoms at high temperature (1000°C) after thinning.[3] However, this process cannot be used with the CCDs employed in this work due to the aluminum metallization. Texas Instruments has developed a process which allows this accumulation to be accomplished without the use of high temperatures after metallization. This process has been shown to be capable of producing spectral responses which are apparently not degraded by losses at the back surface, except for optical reflection. However, results have varied from device to device as shown in Figure 12. Measurements were made, as described below, to characterize this process, with the goals of reproducibility of spectral response and determining the effects of the process on dark currents.

2. Measurement Techniques

The accumulation process was characterized with respect to its most critical variable "α," a controllable variable. The process was characterized by processing a device with sequential, monotonic changes in α, monitoring the device dark current and photoresponse before and after each step. To facilitate this sequential processing, all measurements were made on unmounted chips using a functional multiprobe. This multiprobe consists of a chuck with imbedded light sources for backside illumination and a probe card with individual probes for each bond pad. Electrical signals are supplied to the probes as required to operate the chip.

CCD SPECTRAL RESPONSIVITY

● 1 - Example of High Blue Response Device

▲ 2 - Numerically Averaged Spectral Response of 20 Devices
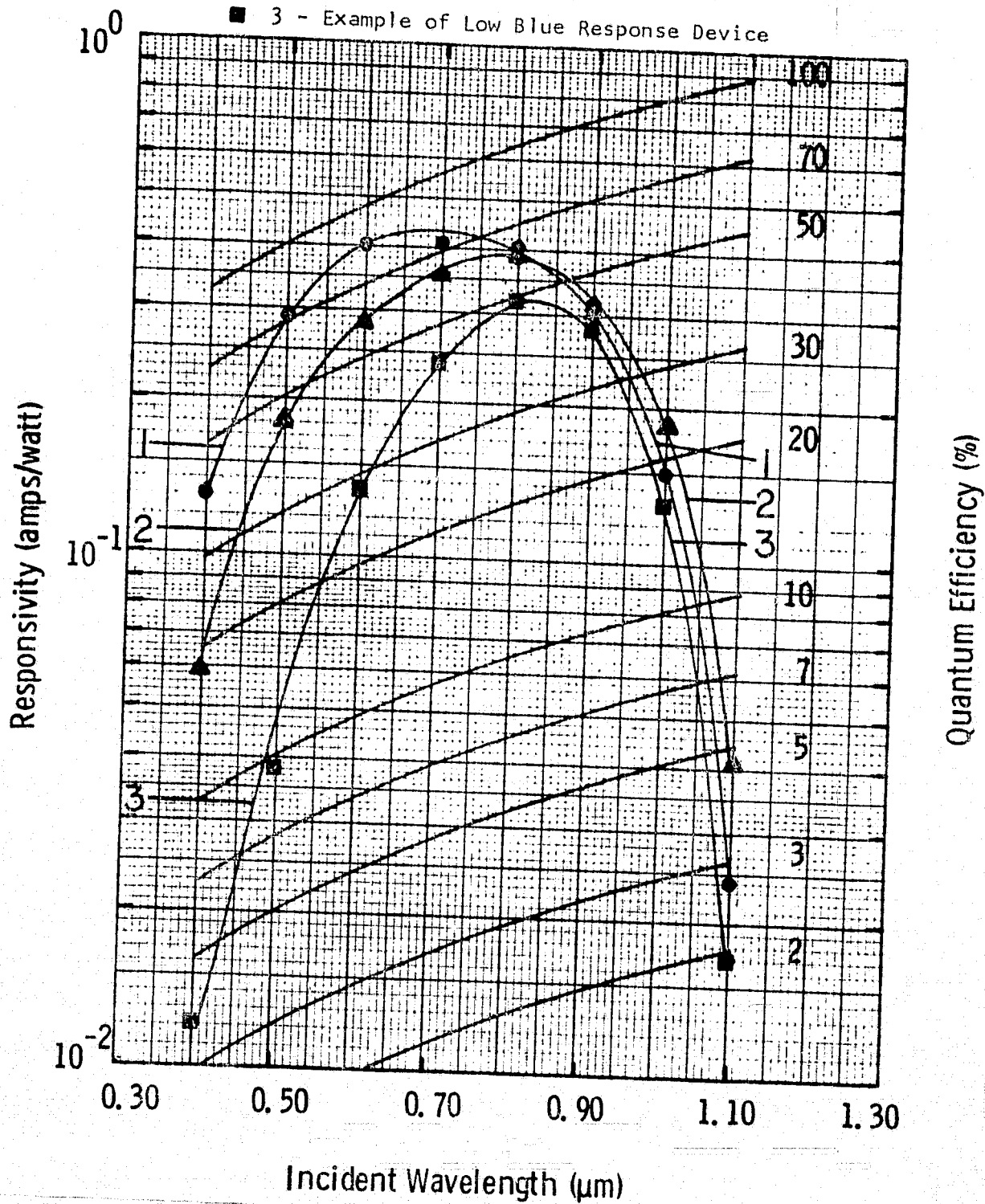
■ 3 - Example of Low Blue Response Device

Figure 12   Summary of Spectral Response Data for Twenty Delivered Devices

3. Measurement Results

The first sets of measurements were made using a green 5600 $\overset{\circ}{A}$ light-emitting diode for photoresponse measurements. Typical results are shown in Figure 13, where dark circles represent the normalized photoresponse at 5600 $\overset{\circ}{A}$ and the Δ's represent the dark current density for sequential values of the variable α.

These data indicate the effectiveness of TI's accumulation process. The photoresponse at 5600 $\overset{\circ}{A}$ is increased by a factor of 550 as a result of this processing. The maximum response observed corresponds approximately to the reflection limit. The data also indicate, however, that the process can have a serious effect on the dark current level. For values of the variable α above an optimum value, the dark current density increases rapidly, and the photoresponse is observed to decrease. Devices processed to this point sometimes display time-dependent dark current and photoresponse.

These data indicate that the variable α must be closely controlled during the accumulation processing at a value that will maximize photoresponse while maintaining the initial dark current level. The bars on the horizontal axis of Figure 13 show the range of values of α typically employed prior to these measurements. These values lead to high photoresponse, but also produce increased dark current.

The reproducibility of these data was investigated by taking other chips and processing them to various values of α. The results are shown in Figure 14. Each open circle indicates a different device. This figure indicates that reproducible spectral responses can be obtained if the variable α is maintained at a value at or below its optimum value.

The light emitting diode was employed initially due to its availability and simplicity of installation in the multiprobe chuck. To further investigate
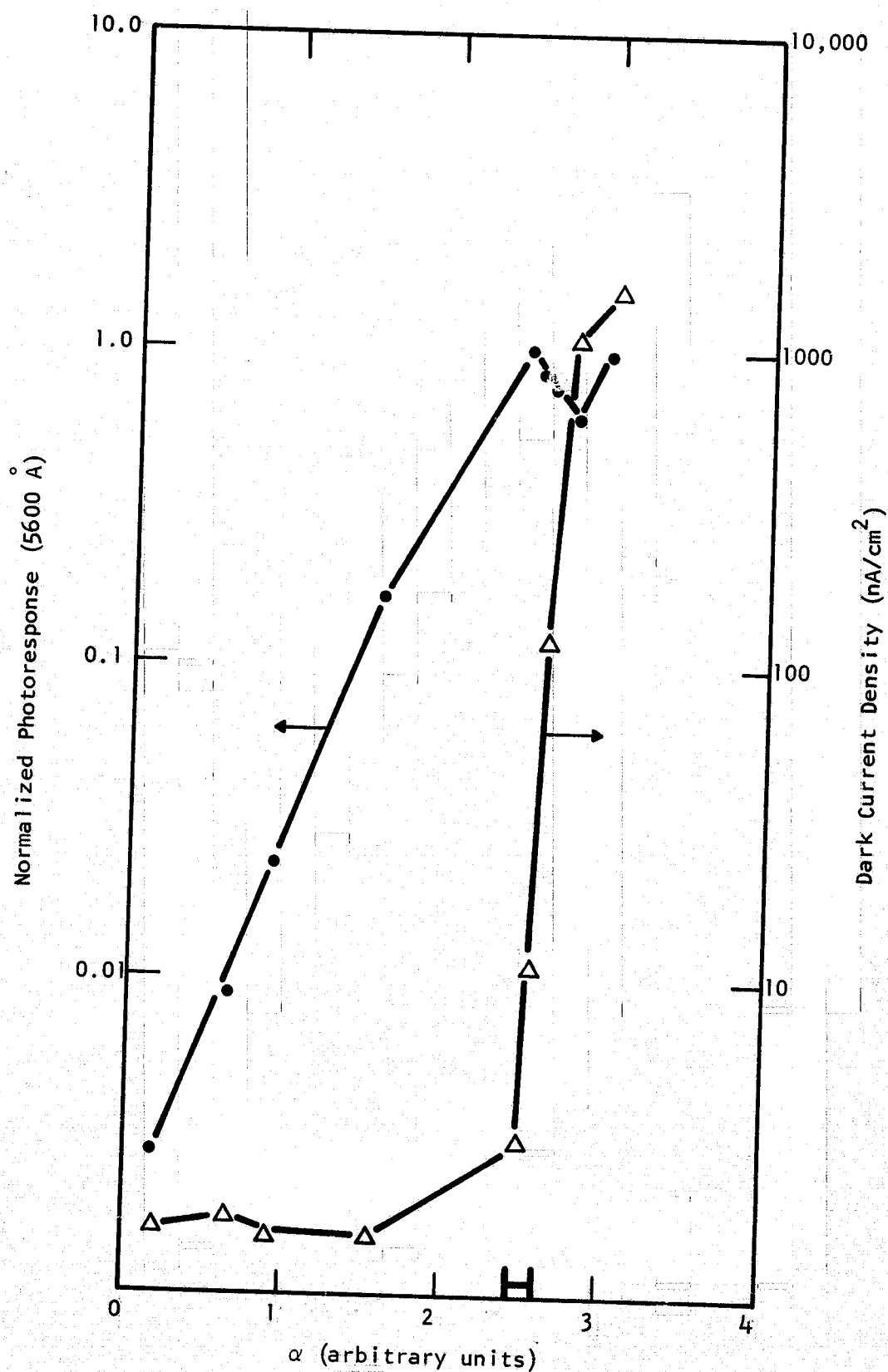
Figure 13 Effects of TI Accumulation Process on Photo-
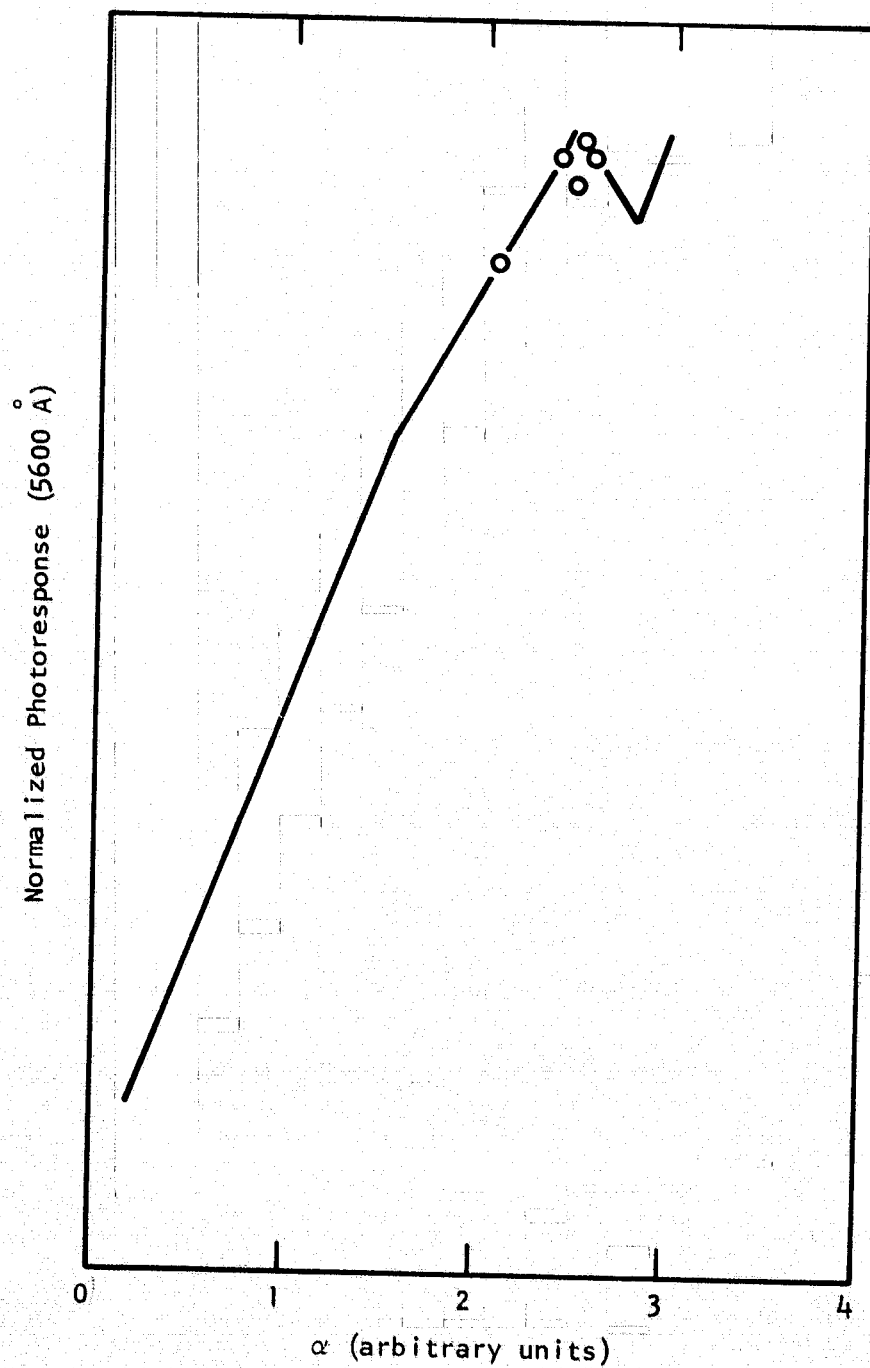response and Dark Current

25

Figure 14   Response Reproducibility of the Tl
Accumulation Process

26

the optimum value of α, it was desirable to use 4000 $\overset{\circ}{A}$ illumination, since this radiation is more sensitive to the backside accumulation layer. This was accomplished by replacing the LED with a fiber optic light pipe. The backside of the chips could then be illuminated with photons of any wavelength through the use of narrowband optical filters between the light source and the input to the light pipe.

Figure 15 shows results obtained using the light pipe. Data on green response (5461 $\overset{\circ}{A}$), blue response (4000 $\overset{\circ}{A}$), and dark current for a single device are presented for sequential values of α. Incremental steps are smaller in these data than in Figure 13 so that the optimum value of α can be defined more precisely.

Two important results are indicated in Figure 15:

(1) Although the blue response and the green response show similar behavior, the blue response peaks at a lower quantum efficiency ($\sim 20\%$) than the green response ($\sim 70\%$); and

(2) The maximum blue response occurs at the onset of dark current increase.

The magnitude of the blue response peak is a function of other variables in the process which are normally held constant. Internal investigations are being made to determine the causes of this blue response limit. The increase in dark current can be avoided by choosing a value of α somewhat below the value for peak blue response.

These results were immediately applied to device processing. Reproducible spectral response curves have been obtained, and dark current increases during the accumulation process have been eliminated. Typical data are presented in Figure 16, showing spectral data for six recently processed devices.

27
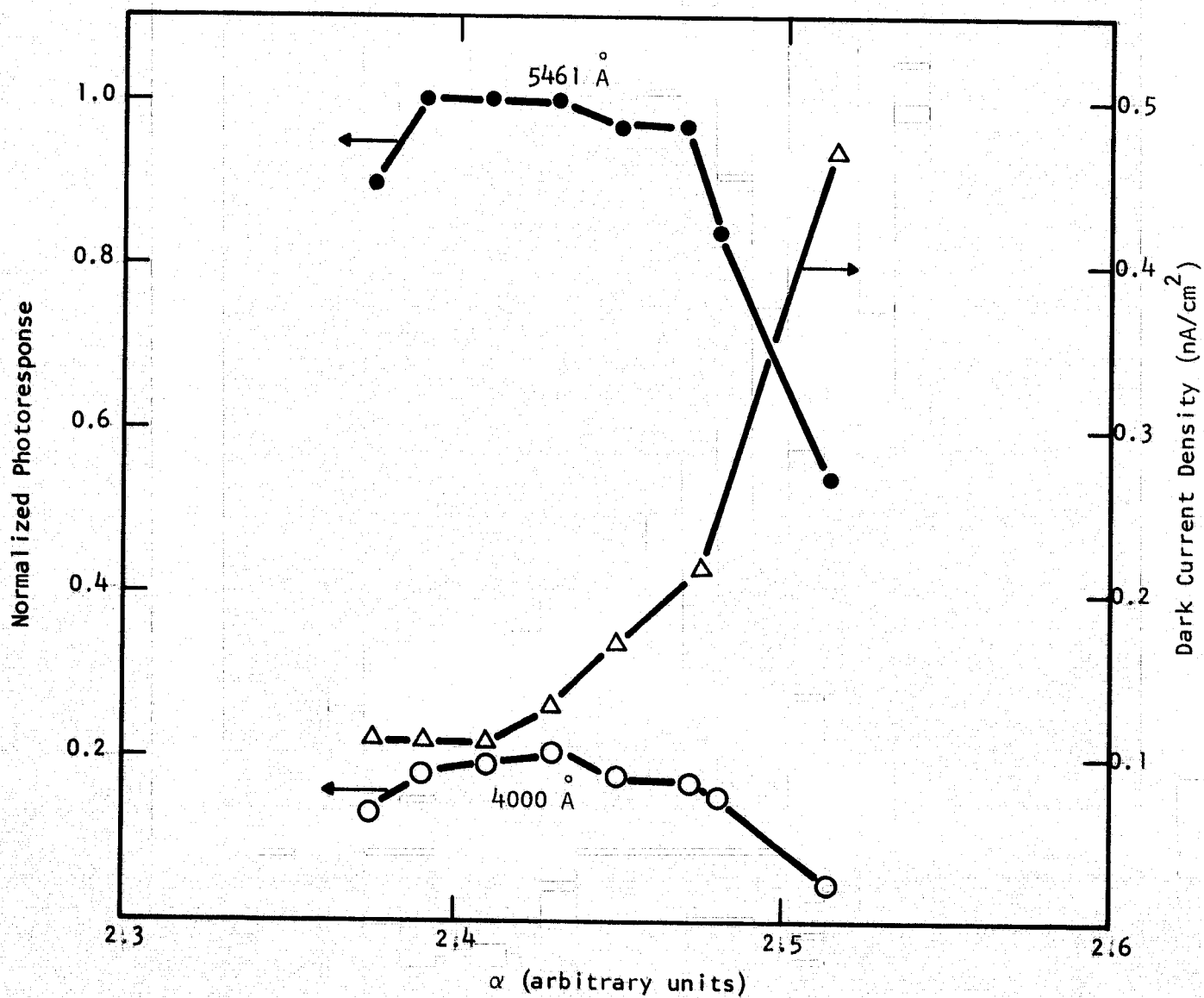
Figure 15 Optimization Data for the Tl Accumulation Process

28
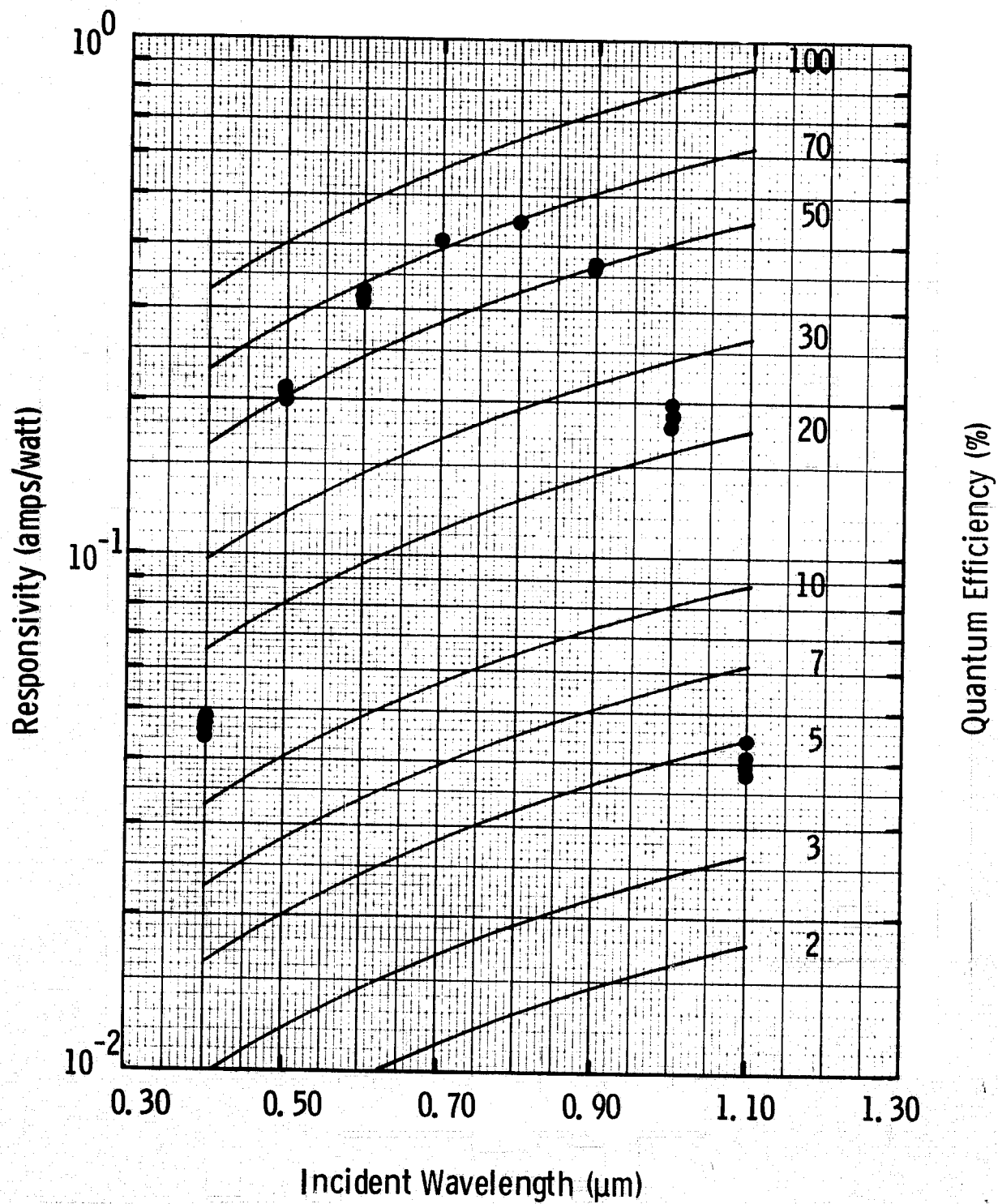
Figure 16   Spectral Response of Six Recent Devices

4. Conclusions

The accumulation process has been characterized with respect to its most critical variable. The results indicate that reflection-limited response can be reproducibly obtained above 6000 $\overset{o}{A}$. Dark current increases during the accumulation process have been discovered and eliminated. The blue response is limited to about 15% to insure low dark current and stability.

SECTION III
DEVICE DELIVERIES

A. **CCD Characteristics**

Four ICCDs were delivered under this contract. The CCDs selected for these devices were characterized before and after tube processing. Performance goals for the CCDs were as follows:

	Medium	High
Transfer Efficiency	> 0.999	> 0.9999
Functional Area for Imaging	> 90%	> 95%
Dark Current (T = 23°C)	< 18 nA/cm^2	< 12 nA/cm^2
Q.E. (λ = 0.4 μ)	> 10%	> 20%

Two medium-quality and two high-quality arrays were to be committed to tube processing.

Copies of the characterization reports for the four delivered devices are presented in the appendix of this report.

The medium quality devices were numbered 220-18-8 and 220-18-16. The high-quality devices were numbered 284-1-8 and 284-1-9. Significant differences exist in the processing of these sets of devices and in the resulting characteristics. The first two devices were processed prior to the development of the processing improvements detailed in Section III, the second two devices after these improvements.

Spectral response curves for the four devices are compared in Figure 17, illustrating the accomplishments of the process characterization. The response of the earlier devices is depressed compared to the later devices. The earlier devices show the variability of results as illustrated previously in Figure 12. The later devices show the reproducibility illustrated in Figure 16.

31

CCD SPECTRAL RESPONSIVITY

▲ 220-18-8
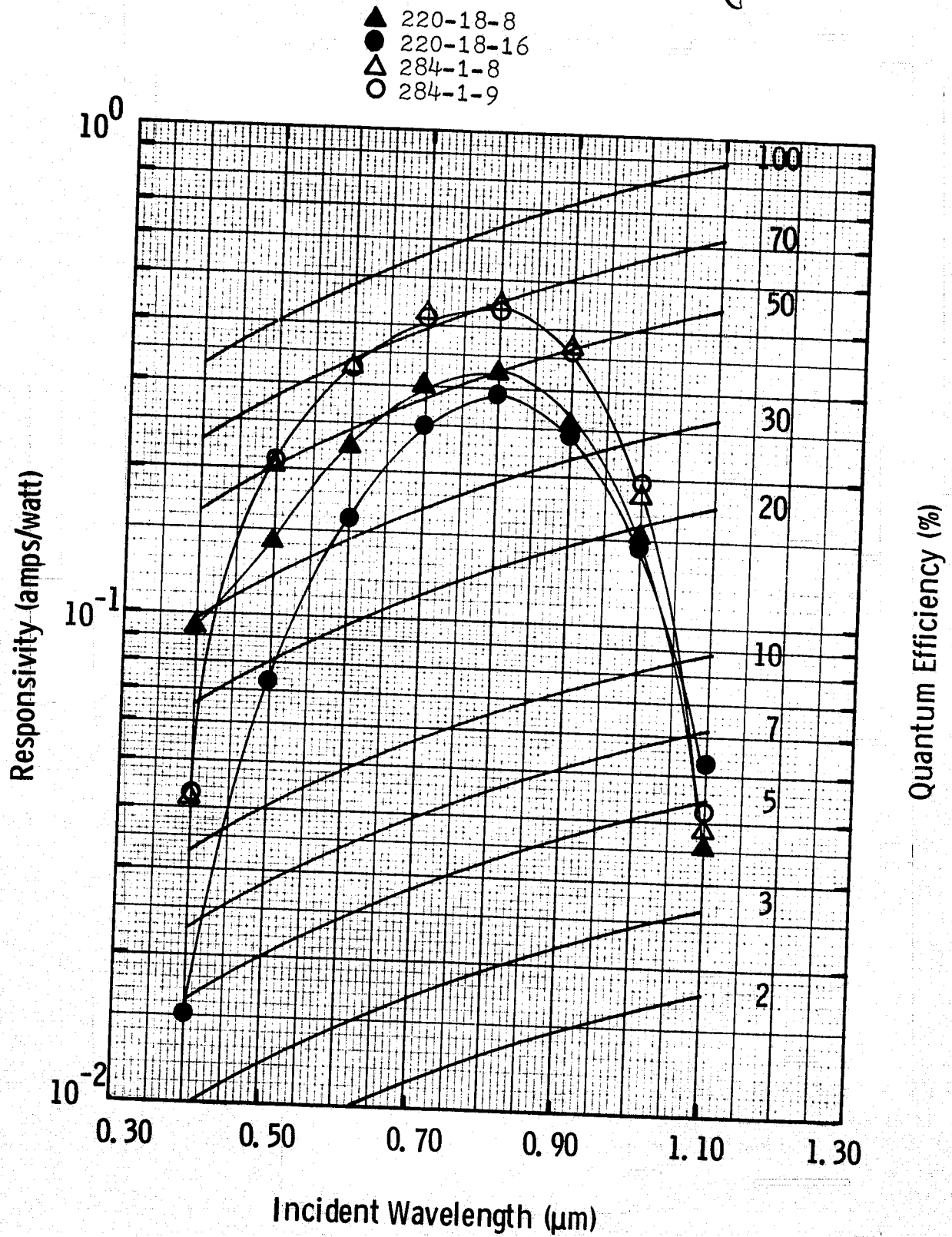● 220-18-16
△ 284-1-8
○ 284-1-9

Figure 17 Spectral Response Comparison of Delivered Devices

Dark current and CTE for the later devices are also superior to the earlier devices. The medium-quality devices had dark currents of 11 nA/cm^2 and 12 nA/cm^2; the high-quality devices had values of 3.6 nA/cm^2 and 4.3 nA/cm^2. The CTE values were 0.9994 and 0.9995 for the medium devices and > 0.99995 for the later devices. Improved uniformity of blue response was also obtained on the later devices, as can be observed from the device reports in the appendix.

The differences between these two device sets are indicative of recent progress in processing of thinned CCD imagers. Devices with characteristics similar to the medium-quality devices no longer result. High-quality devices have been produced infrequently in the past (compare 166-3-2 delivered under Contract No. NAS5-22403), but are now obtained with regularity.

The two sets of devices also had differences in bonding structures. The earlier devices were bonded using aluminum pads and large circumference bonds. The later devices had the protected bond pad structure discussed earlier. No variations in CCD performance prior to tube processing were attributable to this bonding difference.

B.   Tube Processing Results

Tube processing was performed at Varo Electron Devices, Inc., which is located approximately ten miles from TI's Central Research Laboratories in Dallas. The tube processing consisted of four main steps: (1) heliarc weld the tube header to the tube body, (2) evacuate the tube body and bake at 350°C for 10 to 20 hours, (3) process the photocathode, and (4) seal the tube. After processing, the ICCDs were characterized for dark current, imaging capability, and photocathode response. Detailed characteristics of each tube are presented with the CCD data in the appendix.

Tube processing has typically caused dark current increases. This also occurred for these four tubes. Dark current data before and after tube

processing is summarized in Table 2. The data indicate no significant difference between the two sets of devices with regard to tube-processing-induced dark current changes. However, the behavior of the two later devices is not typical of tube processing results obtained since the improvements were made in the accumulation processing. Tubes produced for other programs have typically resulted in 0 to 50% increases in dark current after similar tube processing. Two recent 250 x 400 devices processed under NASA Contract No. NAS5-22924 actually experienced a dark current decrease during tube processing.

One possible reason for this atypical behavior could be related to the bond pad protection process. (Tubes 278 and 279 are the only two tubes processed to date with protected bond pads.) Although this process causes no immediate dark current increase, latent effects may be generated which, when activated by the tube bake, may generate increased dark current. This possibility will be investigated in future beam lead development.

The photocathode characteristics obtained varied from tube to tube. Broadband response and 8000 Å response were measured for the central portion of the photocathode, corresponding to the active CCD area. Results are summarized in Table 3.

Table 3
Photocathode Characteristics of Delivered Devices

Tube No.	Broadband (2854 K) µA/lumen	8000 Å mA/W
245	240	35
246	190	18
278	410	3
279	270	not measured

These data imply variation in the total response and in the spectral content of the response. One possible contributor to these variations is the infrequent application of the tube processing schedule used to fabricate ICCDs.

34

Table 2

Dark Current Changes During Tube Processing

| Tube # | CCD # | Dark Current (nA/cm^2) | | Changes | | Comments |
		Before	After	nA/cm^2	%	
245	220-18-8	12	33	21	175	
246	220-18-16	11	24	13	118	
278	284-1-9	3.6	10.8	7.2	200	line defect introduced
279	284-1-8	4.3	37	33	770	

Additional characteristics of tube 278 were measured and are presented in
Figures 18, 19, and 20. Photocathode properties are detailed in the first two
figures. Figure 18 shows the measured spectral response of the S-20 photo-
cathode. Peak quantum efficiencies above 20% were obtained. This tube has the
highest white light response obtained with a Varo ICCD. Figure 19 shows the
uniformity of the photocathode as measured by making a spot scan across a
diameter (spot size was approximately 25 μm). The bars indicate the portion
corresponding to the active CCD area. The response dips indicated in Figure
19 would have serious effects on ICCD performance if a larger CCD were employed.
These data were reported to Varo personnel, who modified the processing to
eliminate the effect. Recently processed photocathodes do not display this
nonresponsive ring, uniformities as good as ± 5% being indicated from spot
scan data. Finally, Figure 20 shows the EBS gain measured on Tube 278.

PHOTOCATHODE SPECTRAL RESPONSIVITY

TUBE #____278____
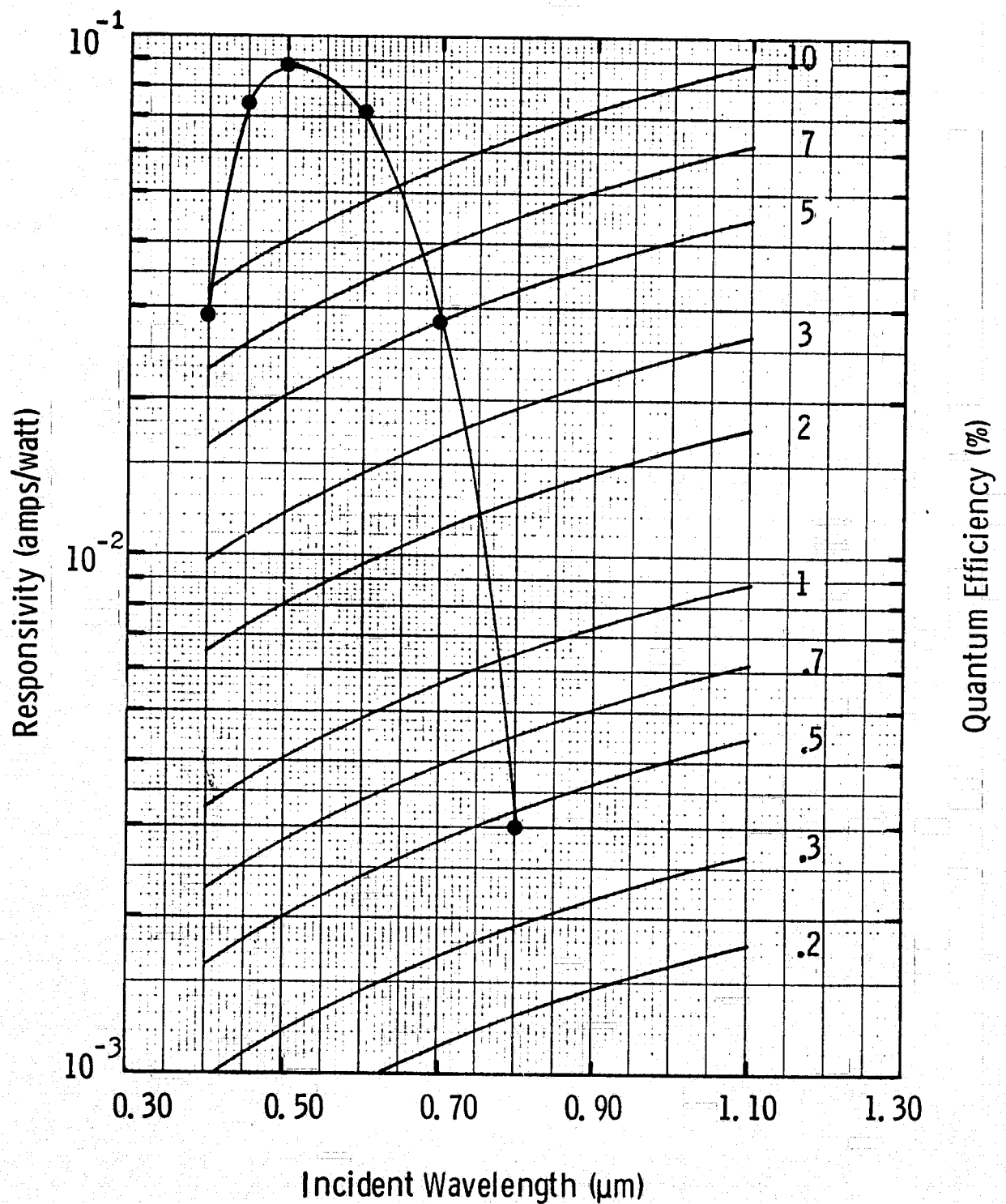

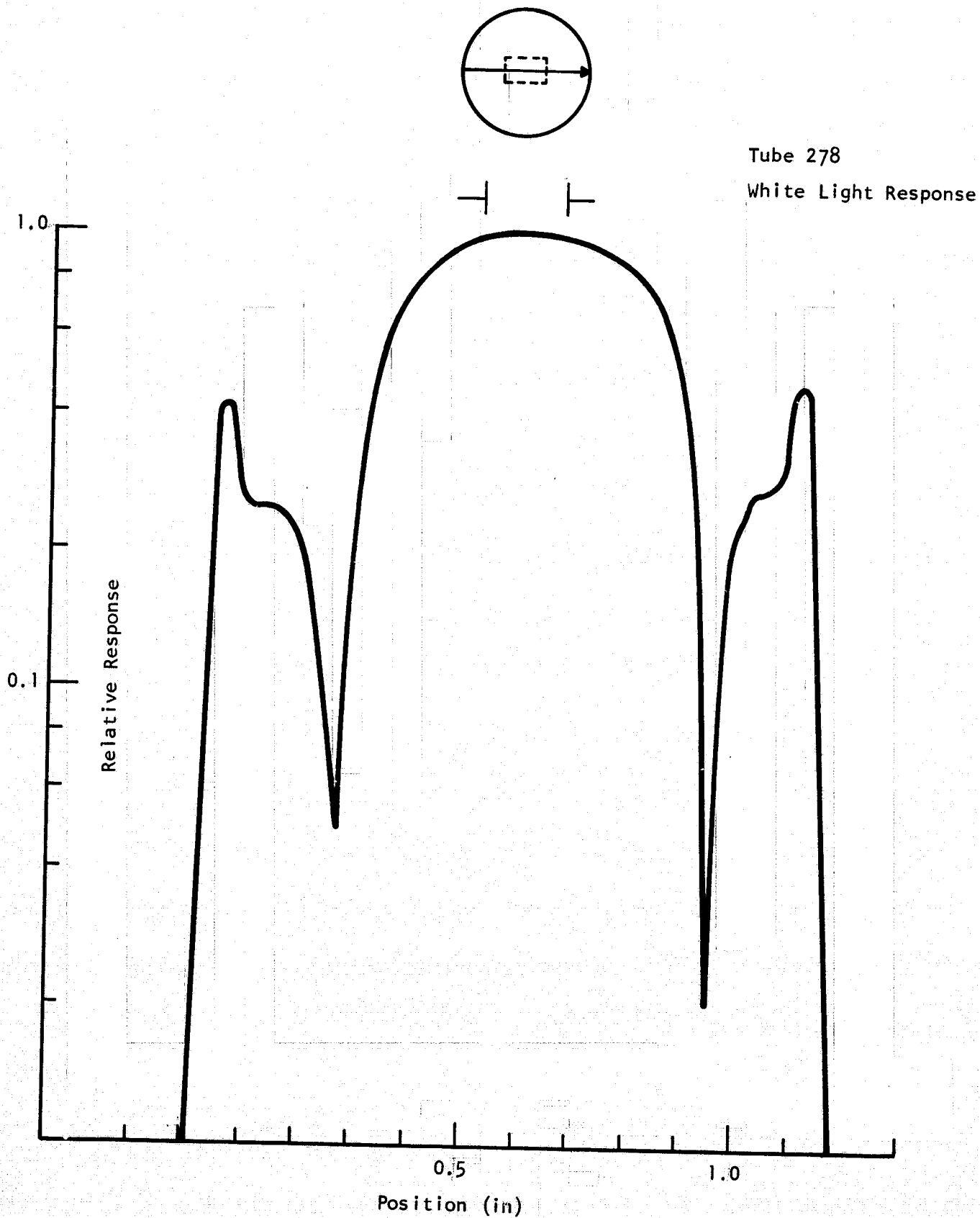Figure 18   Photocathode Spectral Response of Tube #278

Tube 278
White Light Response

Relative Response

Position (in)

Figure 19 Photocathode Uniformity of Tube #278

38

AVERAGE EBS GAIN

CCD Device Number 284-1-9; Tube # 278
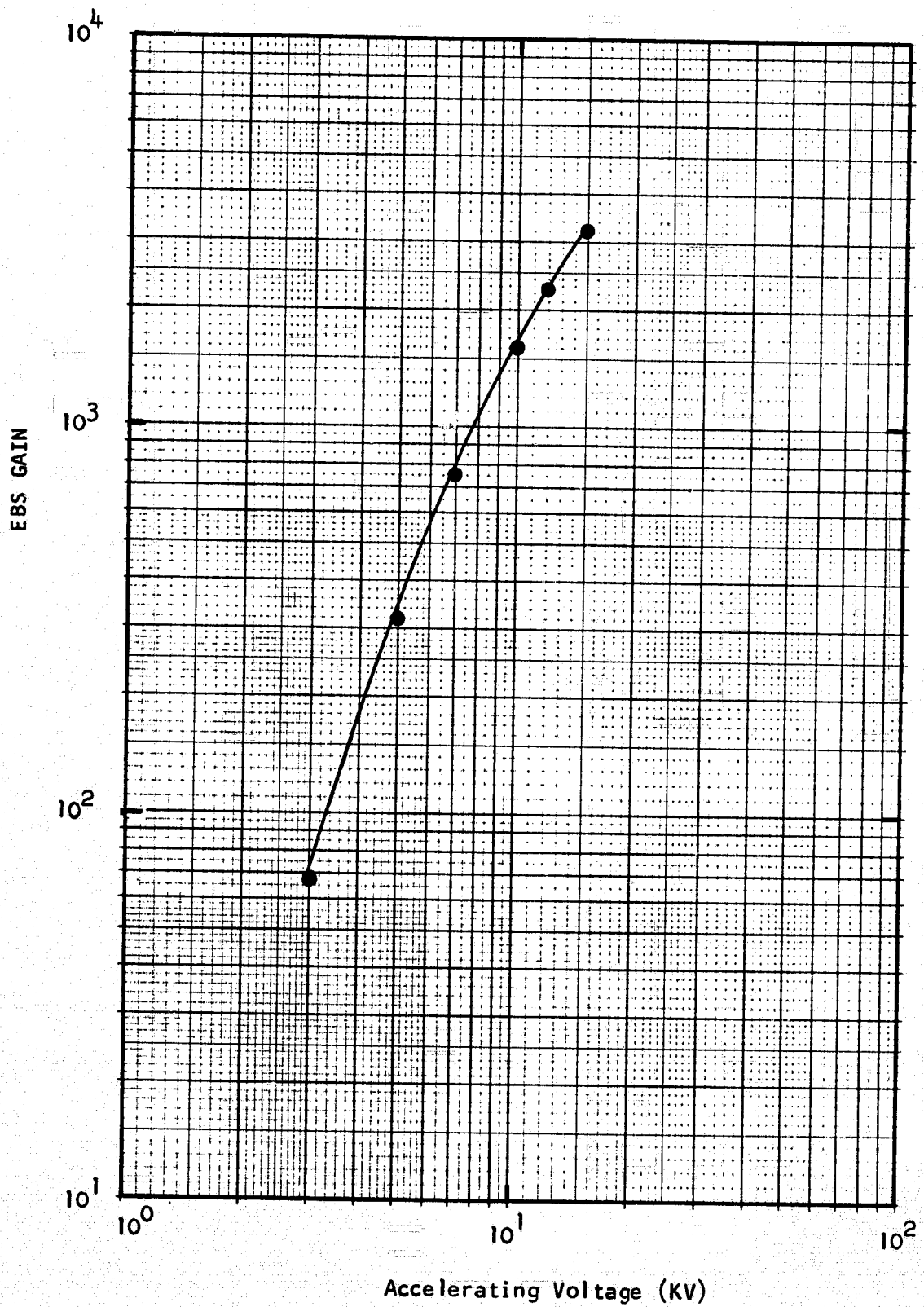

Accelerating Voltage (KV)

Figure 20   EBS Gain of Tube #278

39

SECTION IV
CONCLUSIONS AND RECOMMENDATIONS

Significant progress was made in CCD imager processing for intensified applications during this contract. The accumulation process required for backside illumination has been characterized with respect to the critical variable. Reproducible spectral response characteristics have resulted. Dark current increases due to this process were discovered and eliminated.

A bond pad protection process was developed which eliminated bond strength degradation during tube processing. It was also found that bond failure could be eliminated using gold-to-aluminum bonds if sufficient ball-bond periphery were maintained. This procedure is recommended in the general case because the bond pad protection process requires additional processing time and expense. This process has potential importance, however, as the foundation for beam lead development for CCD imagers.

Four ICCDs were fabricated, characterized, and delivered. The progress made in CCD processing is evidenced by the difference in characteristics between the devices processed before the improvements in the accumulation process and the devices processed after these improvements. The CCDs committed to tube processing met all performance goals with the exception of quantum efficiency at $0.4~\mu$. The lower quantum efficiency results from a tradeoff of quantum efficiency and dark current.

Tube processing has progressed to the point that operational ICCDs are routinely obtained. Future development should lead to further reductions in the dark current introduced by tube processing and to improvements in the photocathode response and uniformity.

REFERENCES

1. T. M. Buck, H. C. Casey, Jr., J. V. Dalton, and M. Yamin, "Influence of Bulk and Surface Properties on Image Sensing Silicon Diode Arrays," Bell Syst. Tech. J. $\underline{47}$, 1827 (1968).

2. E. Philofsky, Solid State Electronics $\underline{13}$, 1391 (1970).

3. S. R. Shortes, W. W. Chan, W. C. Rhines, J. B. Barton, and D. R. Collins, "Characteristics of Thinned Backside-Illuminated Charge-Coupled Device Imagers," Appl. Phys. Lett. $\underline{24}$, 565 (1974).

APPENDIX
Characterization Data for Delivered Devices

CENTRAL RESEARCH LABORATORIES

ICCD Characterization Report

for

NASA/Goddard Space Flight Center
Contract No. NAS5-23578
Device No. 220-18-8 Tube #245

1. CCD DEVICE NUMBER ___220-18-8___

2. DEVICE TYPE ___100 x 160___

   Header type ___tube header with Varo flange___

   Active area __0.0836__ cm^2, pixel dimensions __0.9__ mils X __0.9__ mils

3. OPERATING LEVELS in volts

SUBS (substrates)		
P CLK (parallel clocks)	__-1__	V_{ref} (precharge reference) __18__
S CLK (serial clocks)	__15__	V_{dd} (drain voltage) __21__
SID (serial input diode)	__15__	V_{gg} (load bias)
SOG (serial output gate)	__30__	
V_{pc} (precharge pulse amplitude)	__2__	
	__19__	

4. AMPLIFIER CONFIGURATION used for the tests in this report _____

   ___simple precharge with off-chip load___

5. SPECTRAL RESPONSE

   Quantum efficiency is __28%__ at __0.4__ microns

   __50%__ at __0.8__ microns

   __4%__ at __1.1__ microns.

   Frame readout mode, non shuttered, data rate __1.0__ MHz, frame time __32__ ms, temperature __24__ $^\circ$C, average well population __50__ %.

   Note that quantum efficiencies are uncorrected for reflection.

6. DARK CURRENT

   Dark current measured by precharge current technique is __4.2x10^5__ electrons/pixel/sec (__12__ nanoamps/cm^2) at T = __24__ $^\circ$C.

   Frame readout mode, data rate __1.0__ MHz, frame time __32__ ms.

7. EBS GAIN

   Average EBS gain is _____ at __10__ KV.

8. Charge Transfer Efficiency at 1.0 Mhz is __0.9995__.

9. Membrane Thickness is __10.2__ microns.

CCD IMAGING PERFORMANCE

Device Number 220-18-8   Device Type 100 x 160

Light Source strobe °K Spectral filter none microns

Temperature 24 °C Data rate 1.0 MHz
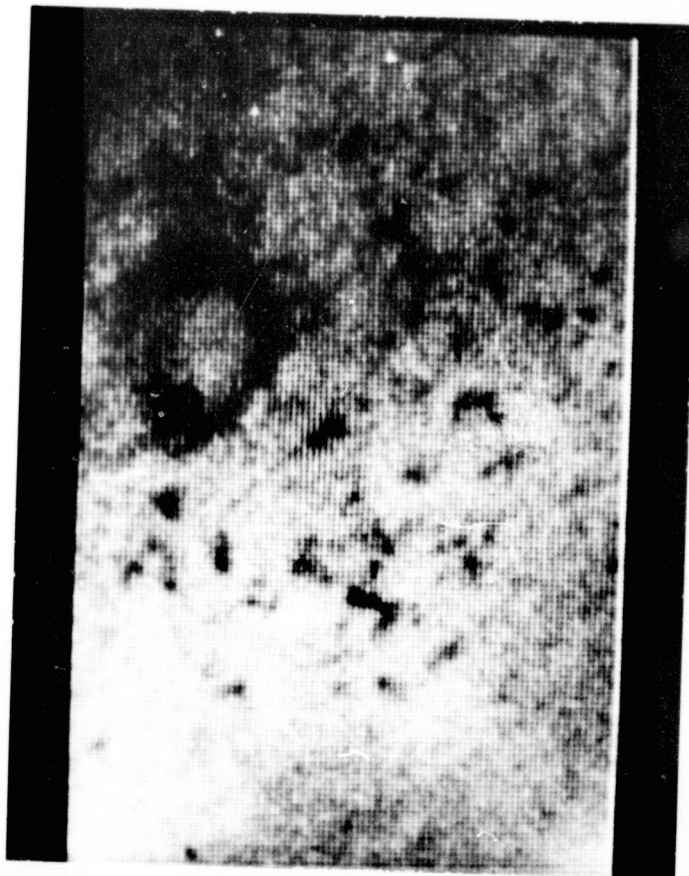
Frame time 32 ms

Device Number __220-18-8__   Device Type __100 x 160__

Light Source __3400__ °K Spectral filter __0.4125__ microns

Temperature __24__ °C Data rate __1.0__ MHz

Frame time __95__ ms

Device Number 220-18-8   Device Type 100 x 160
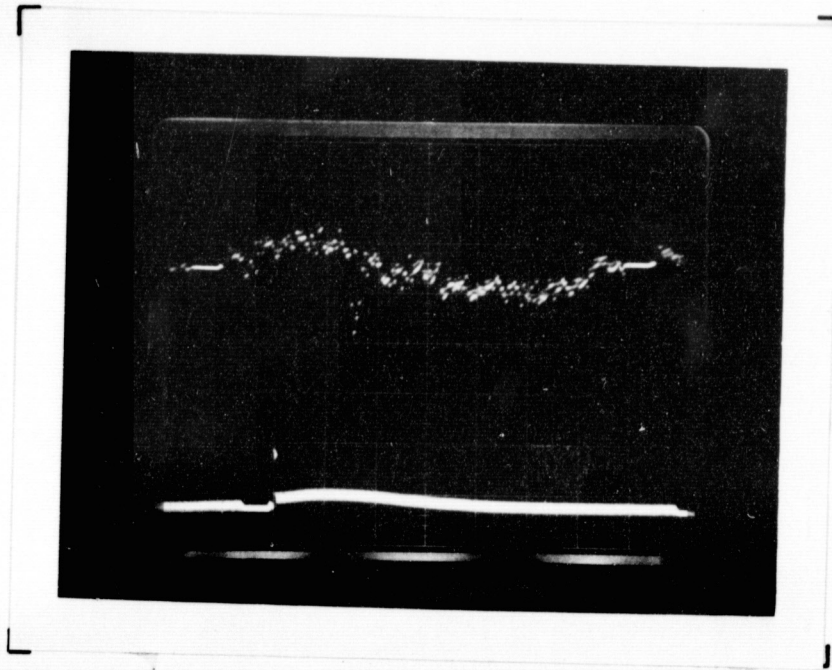

VIDEO MONITOR DISPLAY

Temperature _____24_____ °C

Data rate _____1.0_____ MHz

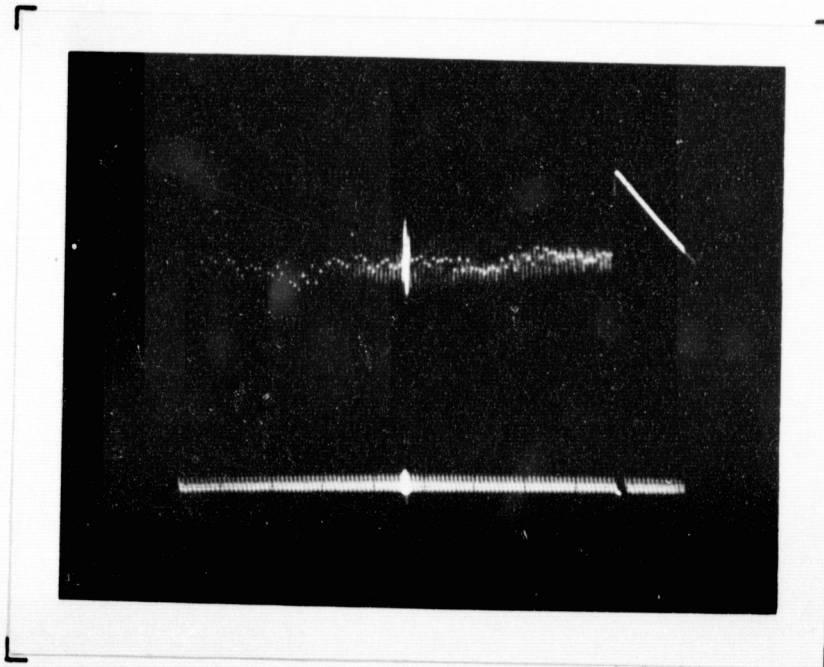Frame time _____1,640_____ ms (50% Full Well)

47

CCD DARK CURRENT UNIFORMITY

Device Number **220-18-8** Device Type **100 x 160**

Temperature **24** °C Data rate **1.0** MHz

Frame time **1,640** ms (50% Full Well)

Oscilloscope presentation

Video line number **50**

Oscilloscope presentation

Complete video frame

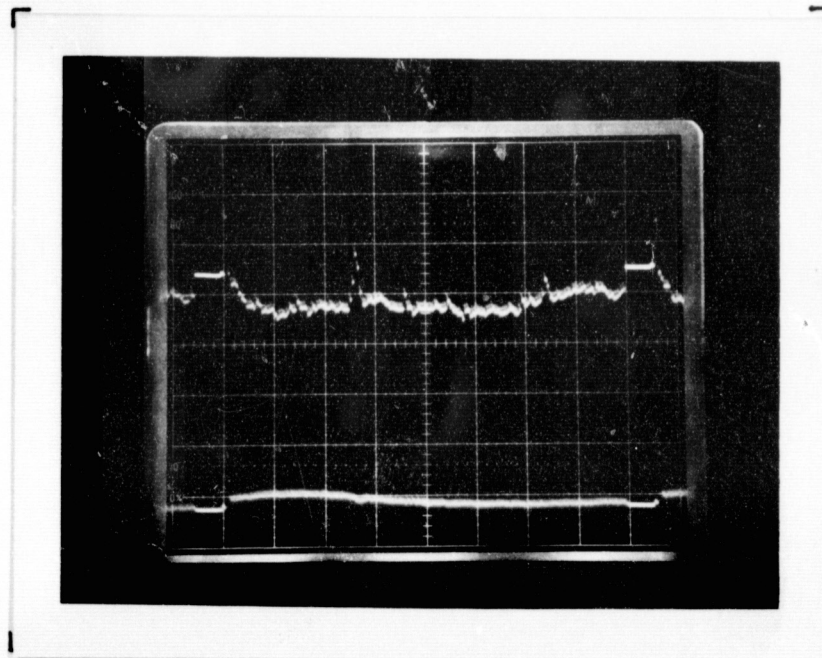Device Number ___220-18-8___   Device Type ___100 x 160___

VIDEO MONITOR DISPLAY

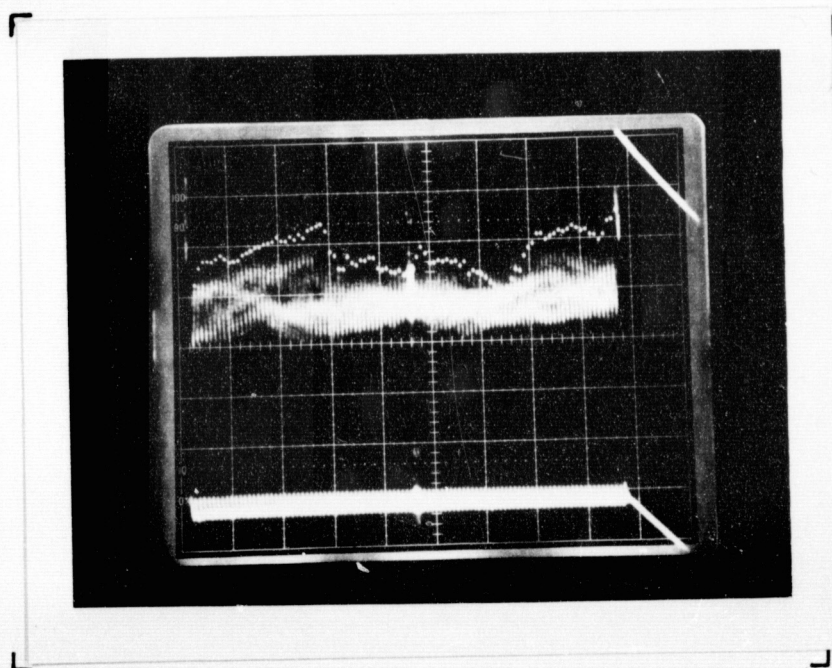|		
Light source	3400	°K
Spectral filter	0.4000	microns
Average well population	50	%
Temperature	24	°C
Data rate	1.0	MHz
Frame time	70	ms

CCD UNIFORMITY OF RESPONSE

Device Number <u>220-18-8</u> Device Type <u>100 x 160</u>

Light source <u>3400</u> °K Spectral filter <u>0.4000</u> microns

Average well population <u>50</u> % Temperature <u>24</u> °C

Data rate <u>1.0</u> MHz Frame time <u>70</u> ms
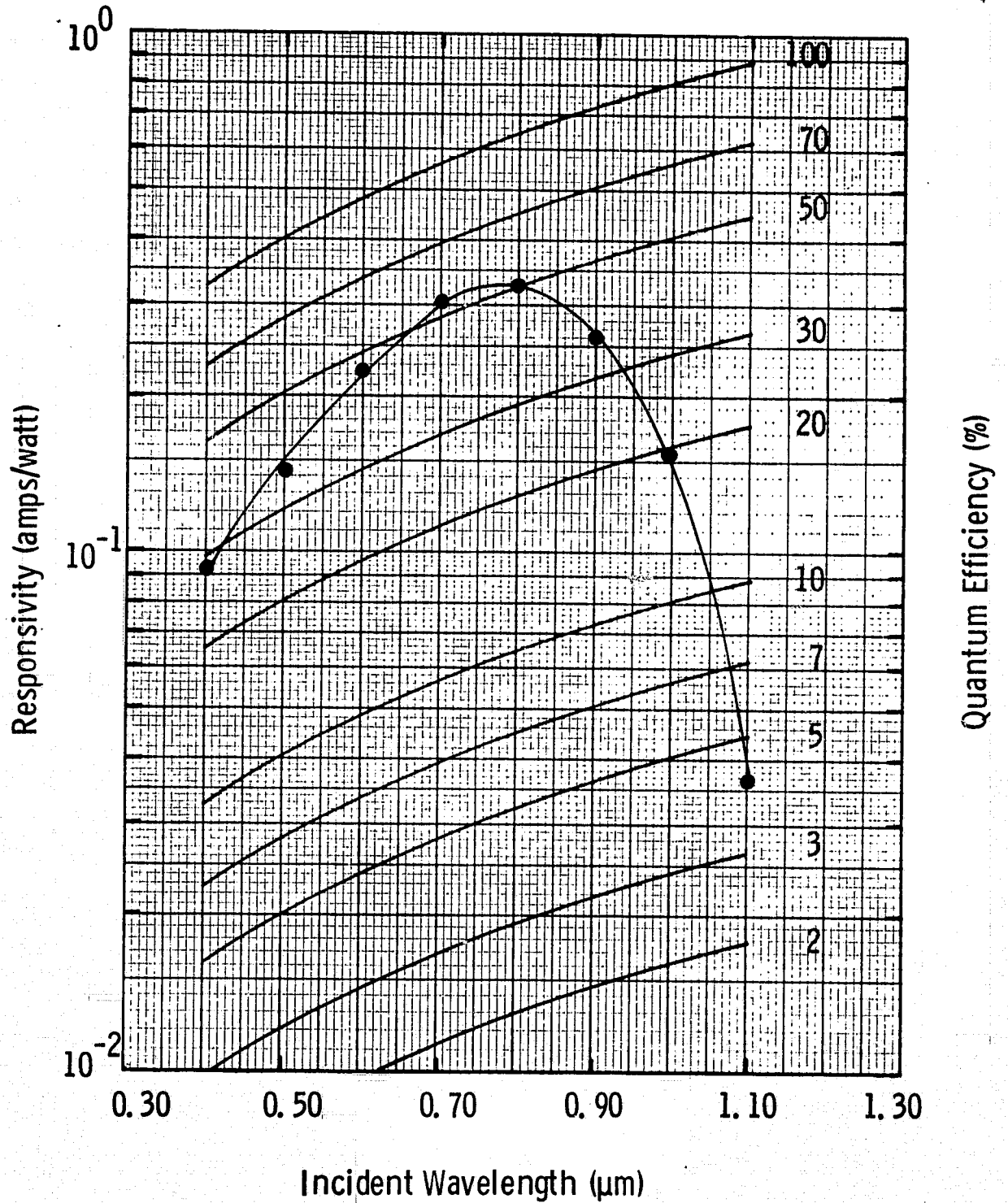

Oscilloscope presentation
Video line number <u>50</u>

Oscilloscope presentation
Complete video frame

CCD SPECTRAL RESPONSIVITY

Device 220-18-8

Responsivity (amps/watt)

Quantum Efficiency (%)

Incident Wavelength (µm)

DATA RATE	1.0	MHz
FRAME TIME	32	MS
TEMPERATURE	24	°C

51

ICCD CHARACTERISTICS

Tube Number __245__

CCD Number __220-18-8__

1. **Dark Current Changes During Tube Processing**

   Before Processing ____ 12 ____ nA/cm^2

   After Processing ____ 33 ____ nA/cm^2

   Change ____ 21 ____ nA/cm^2 ____ +175 ____ %

2. **Photocathode Response**

	Broadband	8000 Å
Full Faceplate Illuminated	360 $\mu A/lumen$	40 mA/W
Central 0.16"x0.10" Illuminated	240 $\mu A/lumen$	35 mA/W

3. **Pin Functions**

Pin Number	Function	Pin Number	Function
1	substrate	17	OP/G^L
2	ϕ_1^U	18	ϕ_{PC}^L
3	ϕ_3^U	19	open
4	ϕ_2^U	20	V_{ref}^L
5	IPG^U	21	open
6	IPD^U	22	open
7	ϕ_T^U	23	OP^L
8	ϕ_3^P	24	open
9	ϕ_2^P	25 *	V_{DD}^L
10	ϕ_1^P	26	OP^U
11	ϕ_T^L	27	open
12	IPD^L	28	open
13	IPG^L	29 *	V_{DD}^U
14	ϕ_2^L	30	OP/G^U
15	ϕ_3^L	31	ϕ_{PC}^U
16	ϕ_1^L	32	V_{ref}^U
		33	substrate

* Note changes in V_{DD} bonding.

52

Device Number 2?0-18-8   Device Type 100x160 EFICCD

Light Source _____ 2854 _____ °K Spectral filter _____ none _____ microns

Temperature _____ 24 _____ °C Data rate _____ 1.0 _____ MHz

Frame time _____ 100 _____ ms

Accelerating Voltage 15.0 KV   Focussing Voltage 14.6 KV

CENTRAL RESEARCH LABORATORIES

ICCD Characterization Report

for

NASA/Goddard Space Flight Center
Contract No.   NAS5-23578
Device No.   220-18-16   Tube #246

CCD OPTICAL AND ELECTRICAL CHARACTERIZATION
TEST REPORT

1. CCD DEVICE NUMBER __220-18-16__

2. DEVICE TYPE __100 x 160__

   Header type __tube header with Varo flange__

   Active area __0.0836__ cm^2, pixel dimensions __0.9__ mils X __0.9__ mils

3. OPERATING LEVELS in volts

SUBS (substrates)	-1	V_{ref} (precharge reference)	18
P CLK (parallel clocks)	15	V_{dd} (drain voltage)	21
S CLK (serial clocks)	15		
SID (serial input diode)	30	V_{gg} (load bias)	
SOG (serial output gate)	2		
V_{pc} (precharge pulse amplitude)	19		

4. AMPLIFIER CONFIGURATION used for the tests in this report

   __simple precharge with off-chip load__

5. SPECTRAL RESPONSE

   Quantum efficiency is __4%__ at __0.4__ microns

   __45%__ at __0.8__ microns

   __4%__ at __1.1__ microns.

   Frame readout mode, non shuttered, data rate __1.0__ MHz,
   frame time __32__ ms, temperature __24__ °C, average well
   population __50__ %.

   Note that quantum efficiencies are uncorrected for reflection.

6. DARK CURRENT

   Dark current measured by precharge current technique is __3.7x10^5__ electrons/
   pixel/sec (__11__ nanoamps/cm^2) at T = __24__ °C.

   Frame readout mode, data rate __1.0__ MHz,
   frame time __32__ ms.

7. EBS GAIN

   Average EBS gain is _____ at __10__ KV.

8. Charge Transfer Efficiency at 1.0 Mhz is __0.9994__ .

9. Membrane Thickness is __10.7__ microns.

CCD IMAGING PERFORMANCE

Device Number __220-18-16__ Device Type __100 x 160__

Light Source __strobe__ °K Spectral filter __none__ microns

Temperature __24__ °C Data rate __1.0__ MHz

Frame time __32__ ms

Device Number 220-18-16 Device Type 100 x 160

Light Source 3400 °K Spectral filter 0.4125 microns

Temperature 24 °C Data rate 1.0 MHz

Frame time 95 ms

Device Number 220-18-16   Device Type 100 x 160

VIDEO MONITOR DISPLAY

Temperature _____ 24 _____ °C

Data rate _____ 1.0 _____ MHz

Frame time _____ 1,640 _____ ms (50% Full Well)

CCD DARK CURRENT UNIFORMITY

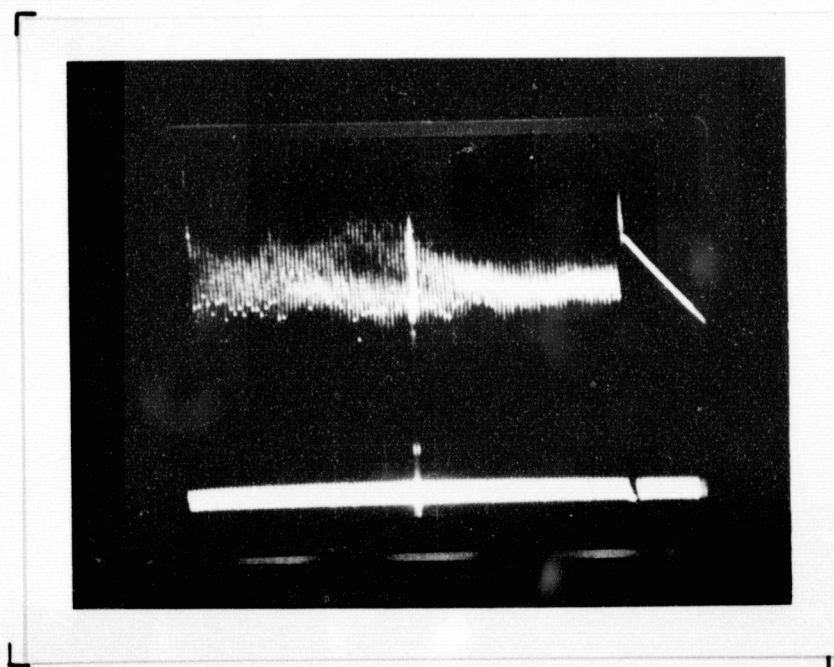Device Number 220-18-16 Device Type 100 x 160

Temperature 24 °C Data rate 1.0 MHz

Frame time 1,640 ms (50% Full Well)

Oscilloscope presentation

Video line number 50

Oscilloscope presentation

Complete video frame

59

Device Number 220-18-16   Device Type 100 x 160

VIDEO MONITOR DISPLAY

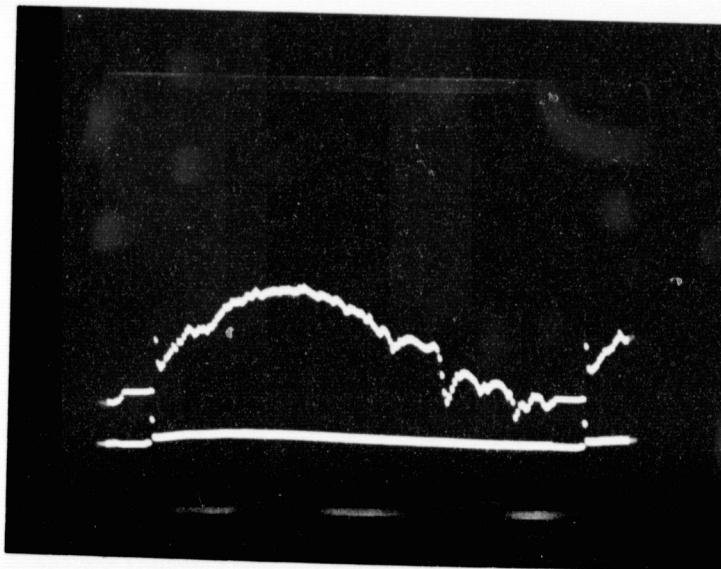|		
Light source	3400	°K
Spectral filter	0.4000	microns
Average well population	50	%
Temperature	24	°C
Data rate	1.0	MHz
Frame time	291	ms

60

Device Number 220-18-16 Device Type   100 x 160

Light source 3400   °K Spectral filter 0.4000 microns

Average well population   50   % Temperature   24   °C
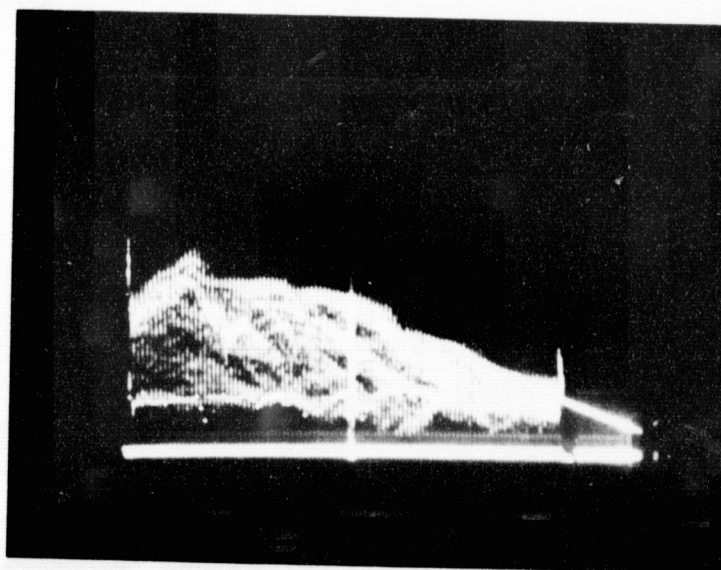
Data rate   1.0   MHz Frame time   291   ms

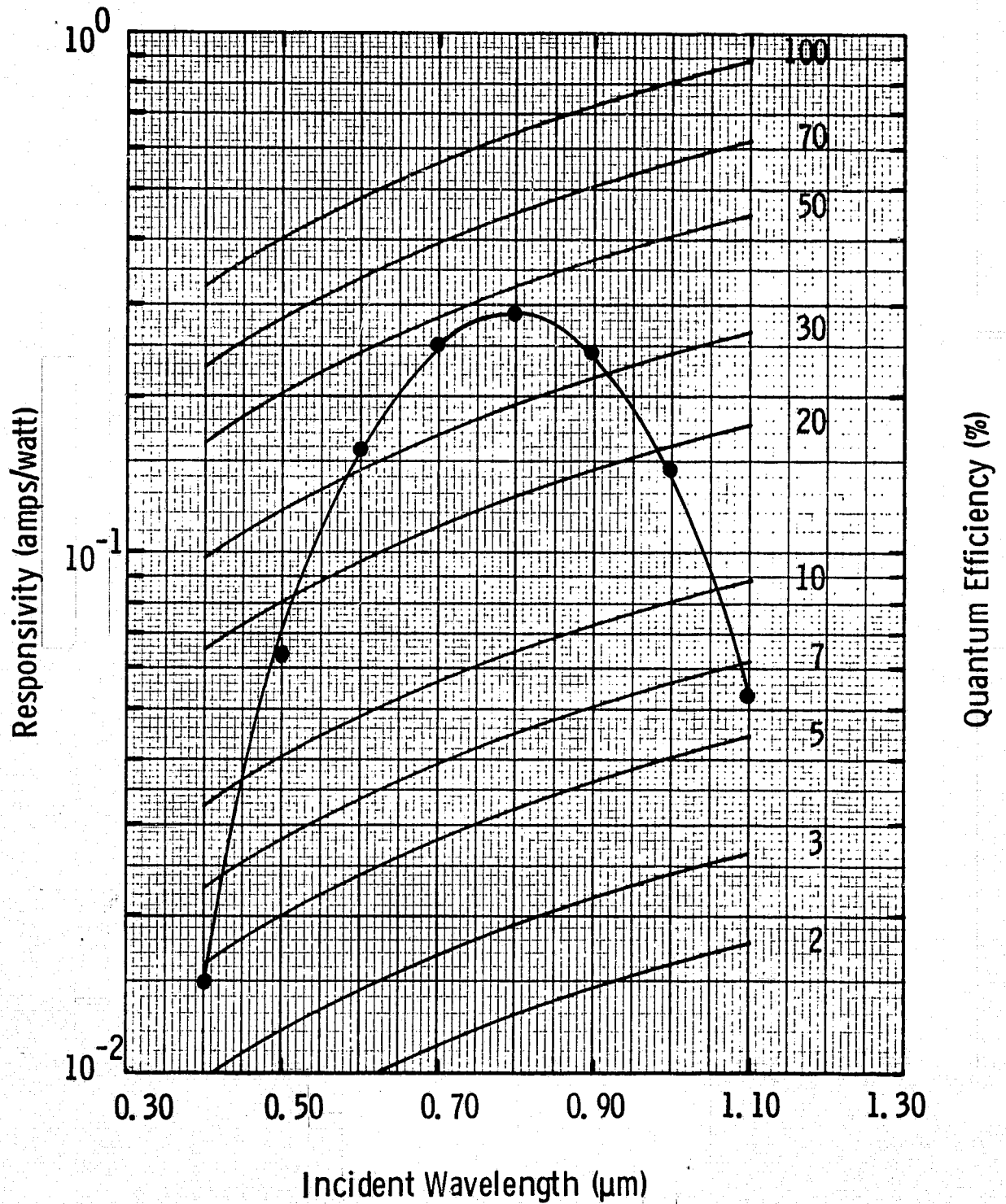Oscilloscope presentation
Video line number   50

Oscilloscope presentation
Complete video frame

61

CCD SPECTRAL RESPONSIVITY

Device 220-18-16

Responsivity (amps/watt) vs. Incident Wavelength (µm), with Quantum Efficiency (%) on the right axis.

DATA RATE   1.0 MHz
FRAME TIME   32 MS
TEMPERATURE 24 °C

ICCD CHARACTERISTICS

Tube Number 246

CCD Number 220-18-16

1. Dark Current Changes During Tube Processing

   Before Processing 11 nA/cm^2

   After Processing 24 nA/cm^2

   Change 13 nA/cm^2 +118 %

2. Photocathode Response

	Broadband	8000 $\overset{o}{A}$
Full Faceplate Illuminated	310 μA/lumen	32 mA/W
Central 0.16"x0.10" Illuminated	190 μA/lumen	18 mA/W

3. Pin Functions

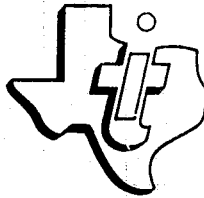 | Pin Number | Function | Pin Number | Function |
   |------------|----------|------------|----------|
   | 1 | substrate | 17 | OP/G^L |
   | 2 | ϕ_1^U | 18 | ϕ_{PC}^L |
   | 3 | ϕ_3^U | 19 | open |
   | 4 | ϕ_2^U | 20 | V_{ref}^L |
   | 5 | IPG^U | 21 | open |
   | 6 | IPD^U | 22 | open |
   | 7 | ϕ_T^U | 23 | OP^L |
   | 8 | ϕ_3^P | 24 | open |
   | 9 | ϕ_2^P | 25 * | V_{DD}^L |
   | 10 | ϕ_1^P | 26 | OP^U |
   | 11 | ϕ_T^L | 27 | open |
   | 12 | IPD^L | 28 | open |
   | 13 | IPG^L | 29 * | V_{DD}^U |
   | 14 | ϕ_2^L | 30 | OP/G^U |
   | 15 | ϕ_3^L | 31 | ϕ_{PC}^U |
   | 16 | ϕ_1^L | 32 | V_{ref}^U |
   | | | 33 | substrate |

* Note Changes in V_{DD} Bonding

Device Number 220-18-16   Device Type 100x160 EFICCD

Light Source 2854 °K Spectral filter none microns

Temperature 24 °C Data rate 1.0 MHz

Frame time 100 ms

Accelerating Voltage 15.0 KV   Focussing Voltage 14.6 KV

CENTRAL RESEARCH LABORATORIES
CCD Optical and Electrical
Characterization Test Report

for

Customer NASA/GODDARD SPACE FLIGHT CENTER

Contract No. NAS5-23578

Device No. 284-1-8; Tube #279

Device Type 160 x 100 in Varo 25mm triode

CCD OPTICAL AND ELECTRICAL CHARACTERIZATION
TEST REPORT

1. CCD DEVICE NUMBER 284-1-8

2. DEVICE TYPE 160 x 100 with protected bond pads

    HEADER TYPE tube header with Varo flange

    Active area 0.836 cm^2 , pixel dimensions 0.9 mils X 0.9 mils

3. OPERATING LEVELS in volts

Substrate	-.5	Lower reference	25
Parallel clocks	11	Upper reference	25
Serial clocks	15	Lower drain	32
Input diode	30	Upper drain	32
Output gate	2	Precharge	15

4. AMPLIFIER CONFIGURATION used for the tests in this report:

    simple precharge with external load

5. SPECTRAL RESPONSE (see accompanying graph)

    Quantum efficiency is 12.9 % at 0.4 microns

    73.9 % at 0.7 microns

    22.7 % at 1.0 microns

6. DARK CURRENT measured by the precharge method

    4.3 nanoamps/cm^2 or 1.4x10^5 electrons/pixel/sec

    T = 25 ^{o}C, data rate 1.0 MHz, frame time 32 ms

7. EBS GAIN (SEM measured)

    Average EBS gain is 635 at 10 KV; 1700 at 15 KV

8. AMPLIFIER RESPONSE: _____ external load, _____MHz data rate
       (not measured)
    lower amplifier _____mV/nA

    upper amplifier _____mV/nA

9. CHARGE TRANSFER EFFICIENCY at 1.0 MHz is > 0.99995 .

CCD IMAGING PERFORMANCE
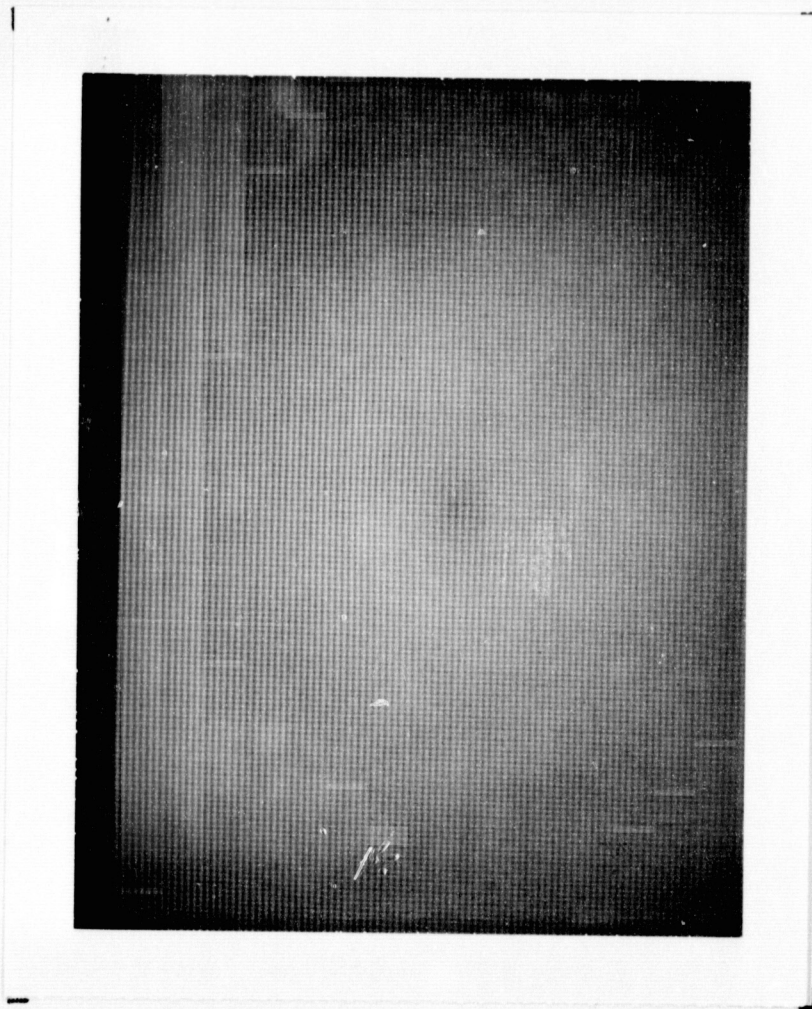
Device Number __284-1-8__   Device Type __160 x 100__

Light Source __strobe__ °K   Spectral filter __none__ microns

Temperature __25__ °C   Data rate __1.0__ MHz

Frame time __32__ ms

CCD DARK CURRENT UNIFORMITY

Device Number 284-1-8   Device Type 160 x 100

VIDEO MONITOR DISPLAY

Temperature _____ 25 _____ °C

Data rate _____ 1.0 _____ MHz

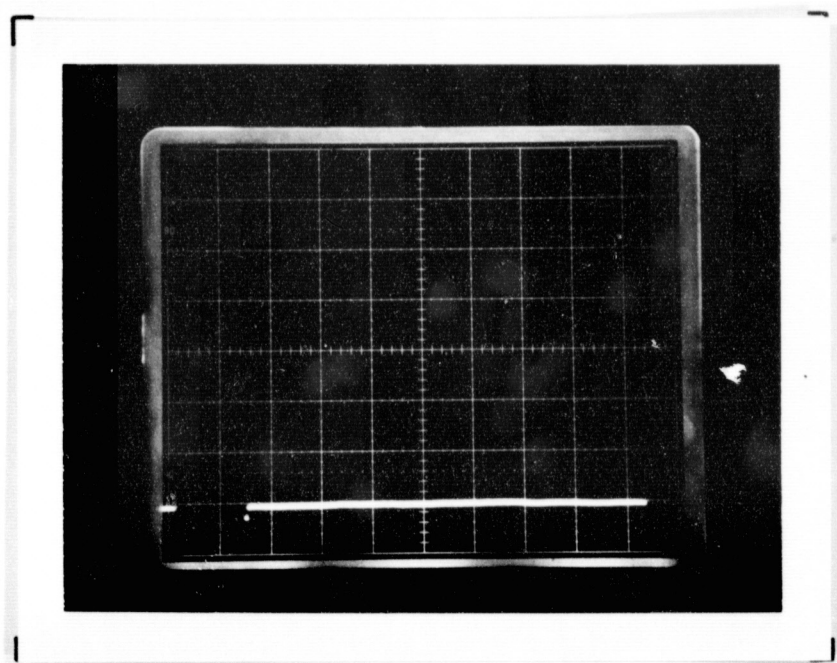Frame time _____ 70 _____ ms

CCD DARK CURRENT UNIFORMITY

Device Number 284-1-8   Device Type   160 x 100
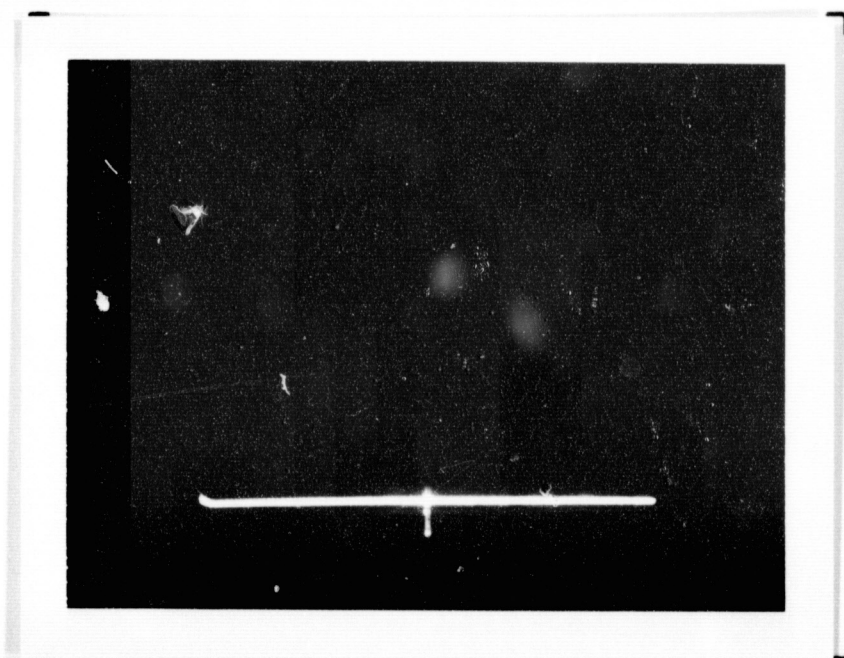
Temperature   25   °C   Data rate   1.0   MHz

Frame time   32   ms

Oscilloscope presentation

Video line number   50

Oscilloscope presentation

Complete video frame
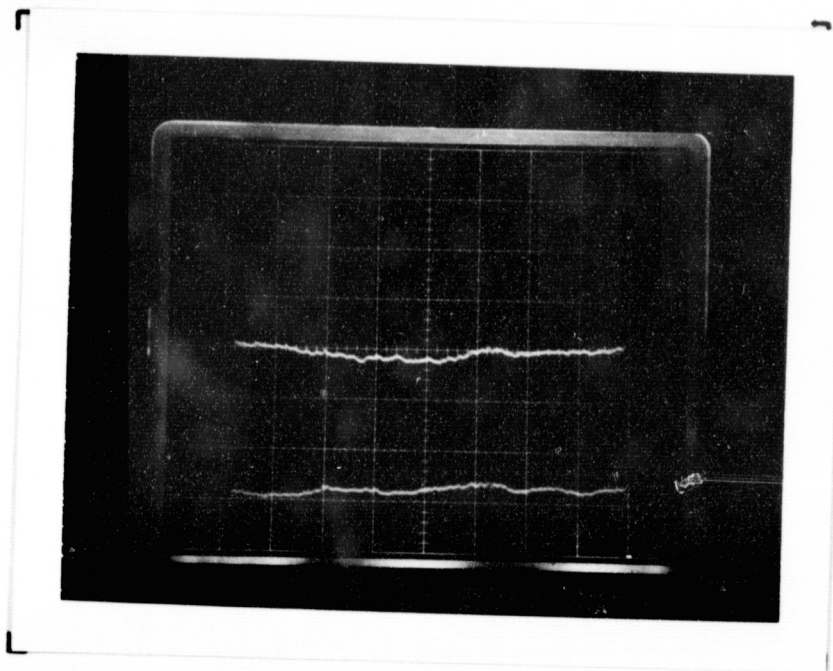
Device Number ___284-1-8___   Device Type ___160 x 100___

VIDEO MONITOR DISPLAY

|		
Light source	3400	°K
Spectral filter	0.4000	microns
Average well population	50	%
Temperature	25	°C
Data rate	1.0	MHz
Frame time	455	ms

CCD UNIFORMITY OF RESPONSE

Device Number 284-1-8 Device Type 160 x 100

Light source 3400 °K Spectral filter 0.4000 microns

Average well population 50 % Temperature 25 °C
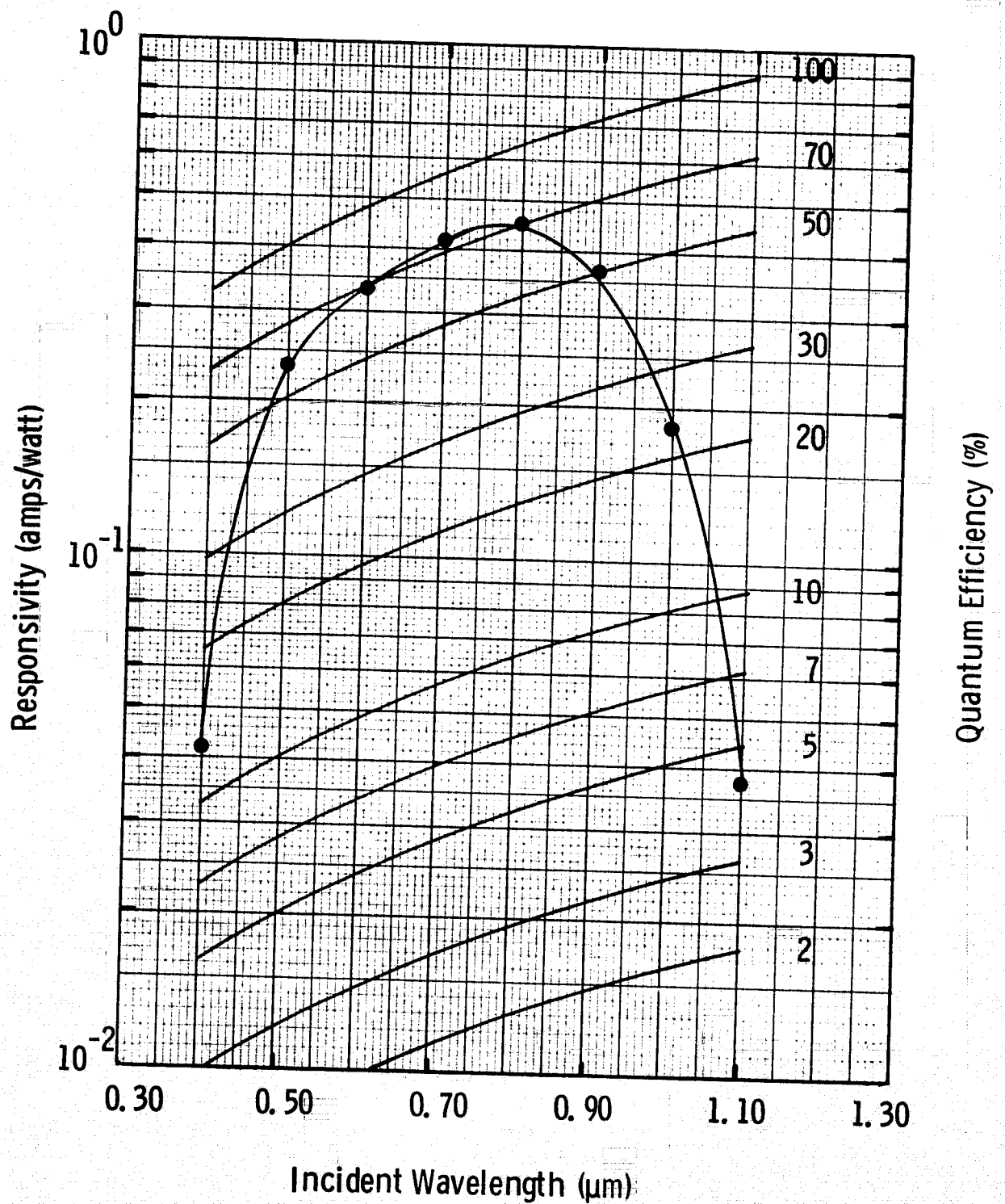
Data rate 1.0 MHz Frame time 455 ms

Oscilloscope presentation
Video line number 50

Oscilloscope presentation
Complete video frame

71
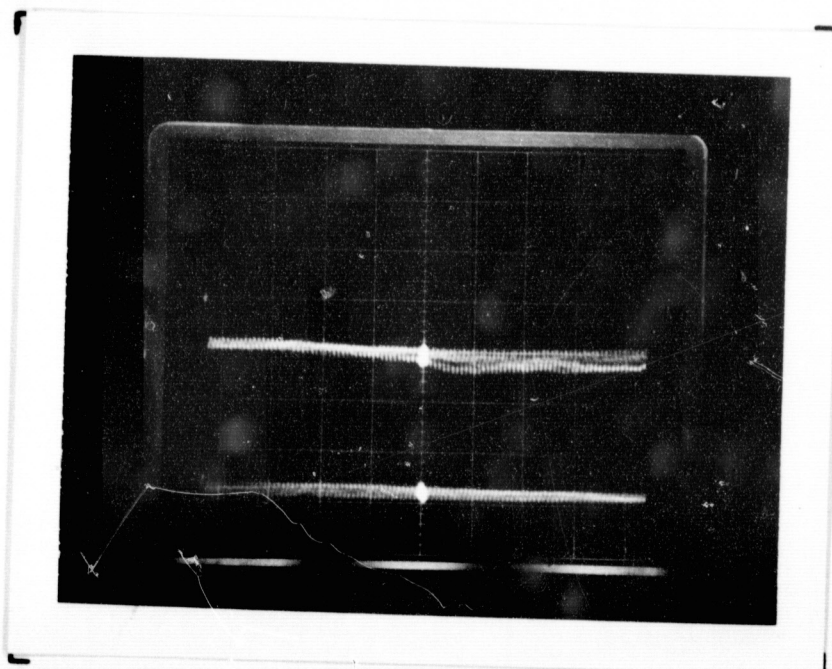
CCD SPECTRAL RESPONSIVITY

Device 284-1-8

Incident Wavelength (μm)

DATA RATE	1.0 MHz
FRAME TIME	32 MS
TEMPERATURE	25 °C

ICCD CHARACTERIZATION REPORT

1. TUBE NUMBER____279_____   DEVICE NUMBER__284-1-8_____

2. MANUFACTURER_Varo Electron Devices_____

   TUBE TYPE___25mm electrostatically-focussed triode_____

3. TUBE PROCESSING EFFECTS

   Dark Current Changes

	Total (nA)	Active Area Density (nA/cm^2)
Before processing	0.51	4.3
After processing	3.38	37

4. PHOTOCATHODE PROPERTIES

   Type_____S20_____

   Responsivity (See accompanying graphs)

   Broadband (2854 K) __270__ A/lm; 8000 A _____mA/W

5. EBS GAIN

   Average EBS gain is _____ at ____KV; _____ at ____KV

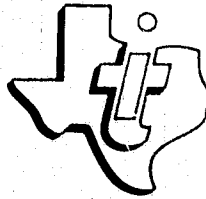6. COMMENTS_____

   _____

   _____

   _____

CCD IMAGING PERFORMANCE

Device Number __Tube #279__ Device Type __160 x 100 Varo Triode__

Light Source __2854__ °K Spectral filter __none__ microns

Temperature __25__ °C Data rate __1.0__ MHz

Frame time __100__ ms Photocathode Illuminance __1.1×10^{-4}__ fc

Accelerating Voltage __15__ KV Focussing Voltage __14.7__ KV

CENTRAL RESEARCH LABORATORIES
CCD Optical and Electrical
Characterization Test Report

for

Customer NASA/GODDARD SPACE FLIGHT CENTER

Contract No. NAS5-23578

Device No. 284-1-9; Tube #278

Device Type 160 x 100 in Varo 25mm triode

CCD OPTICAL AND ELECTRICAL CHARACTERIZATION
TEST REPORT

1. CCD DEVICE NUMBER 284-1-9

2. DEVICE TYPE 160 x 100 with protected bond pads

   HEADER TYPE tube header with Varo flange

   Active area 0.836 cm^2 , pixel dimensions 0.9 mils X 0.9 mils

3. OPERATING LEVELS in volts

Substrate	-.5	Lower reference	25
Parallel clocks	11	Upper reference	25
Serial clocks	15	Lower drain	32
Input diode	30	Upper drain	32
Output gate	2	Precharge	15

4. AMPLIFIER CONFIGURATION used for the tests in this report:

   simple precharge with external load

5. SPECTRAL RESPONSE (see accompanying graph)

   Quantum efficiency is 13.5 % at 0.4 microns

   72.5 % at 0.7 microns

   24.2 % at 1.0 microns

6. DARK CURRENT measured by the precharge method

   3.6 nanoamps/cm^2 or 1.2x10^5 electrons/pixel/sec

   T = 25 °C, data rate 1.0 MHz, frame time 32 ms

7. EBS GAIN (SEM measured)

   Average EBS gain is 890 at 10 KV; 1950 at 15 KV

8. AMPLIFIER RESPONSE: _____ external load, _____ MHz data rate
   (not measured)

   lower amplifier _____ mV/nA

   upper amplifier _____ mV/nA

9. CHARGE TRANSFER EFFICIENCY at 1.0 MHz is > 0.99995 .

Device Number 284-1-9   Device Type 160 x 100

Light Source strobe °K Spectral filter none microns

Temperature 25 °C Data rate 1.0 MHz
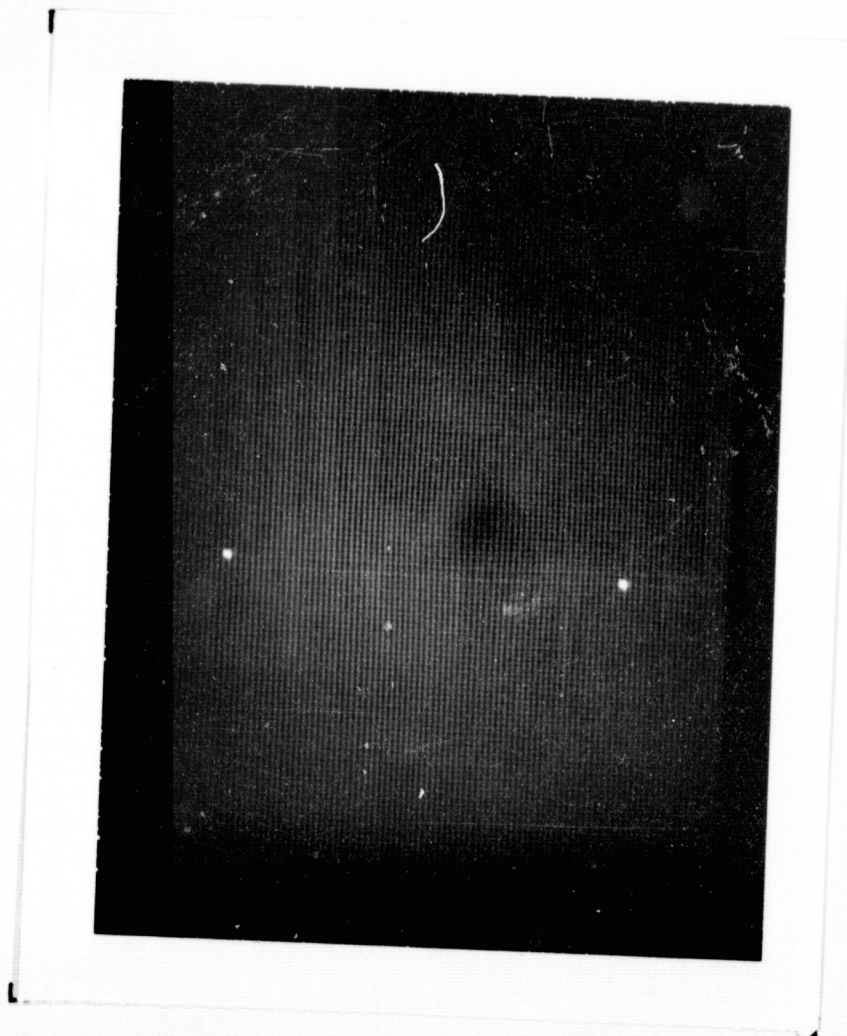
Frame time 32 ms

CCD IMAGING PERFORMANCE

Device Number 284-1-9   Device Type 160 x 100

Light Source _3400_ °K   Spectral filter _0.4000_ microns

Temperature _25_ °C   Data rate _1.0_ MHz

Frame time _430_ ms

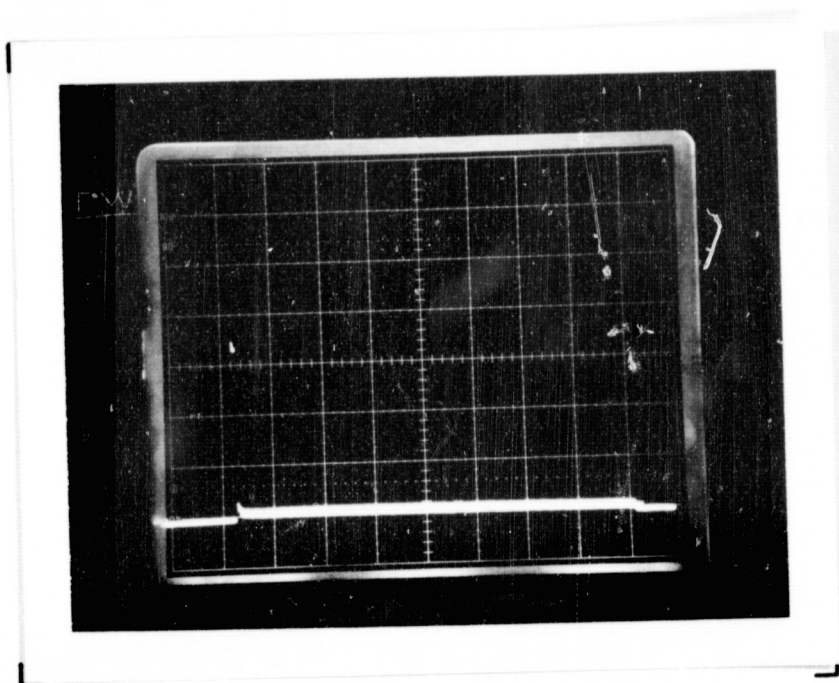Device Number 284-1-9   Device Type 160 x 100

VIDEO MONITOR DISPLAY

Temperature _____25_____ °C

Data rate _____1.0_____ MHz

Frame time _____70_____ ms
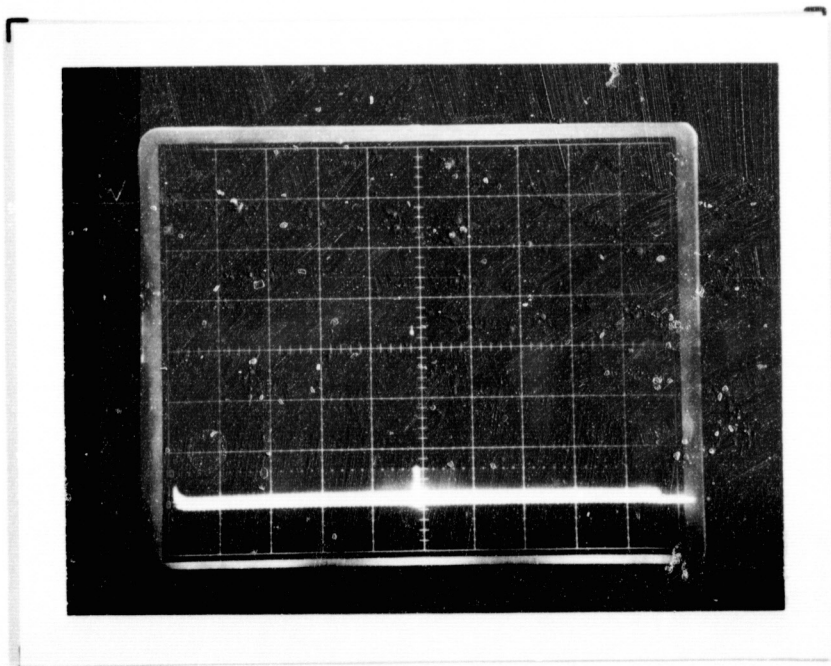
Device Number 284-1-9   Device Type 160 x 100

Temperature 25 °C Data rate 1.0 MHz

Frame time 70 ms

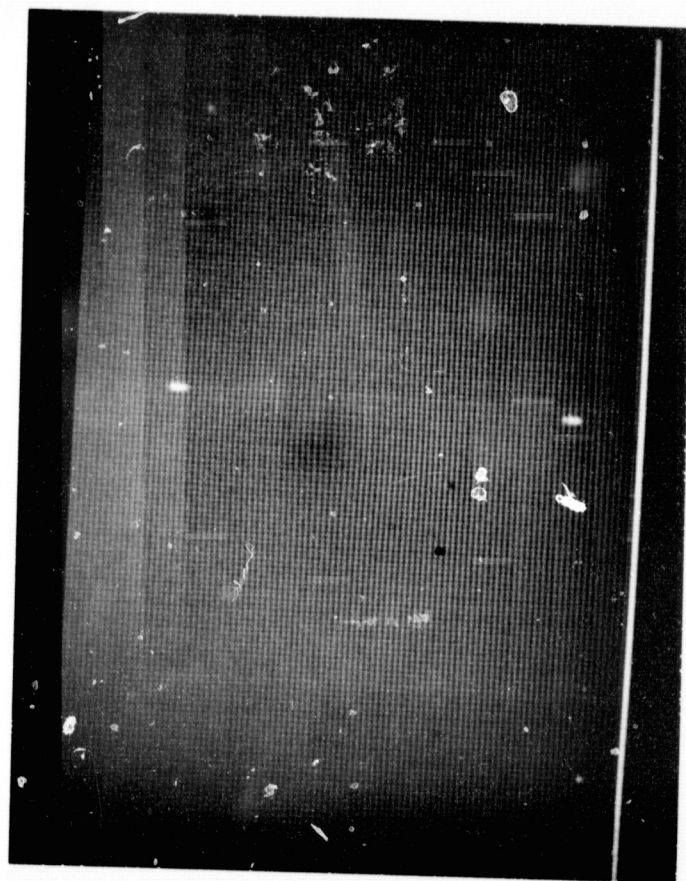

Oscilloscope presentation

Video line number 50

Oscilloscope presentation

Complete video frame

80

Device Number 284-1-9   Device Type   160 x 100

VIDEO MONITOR DISPLAY
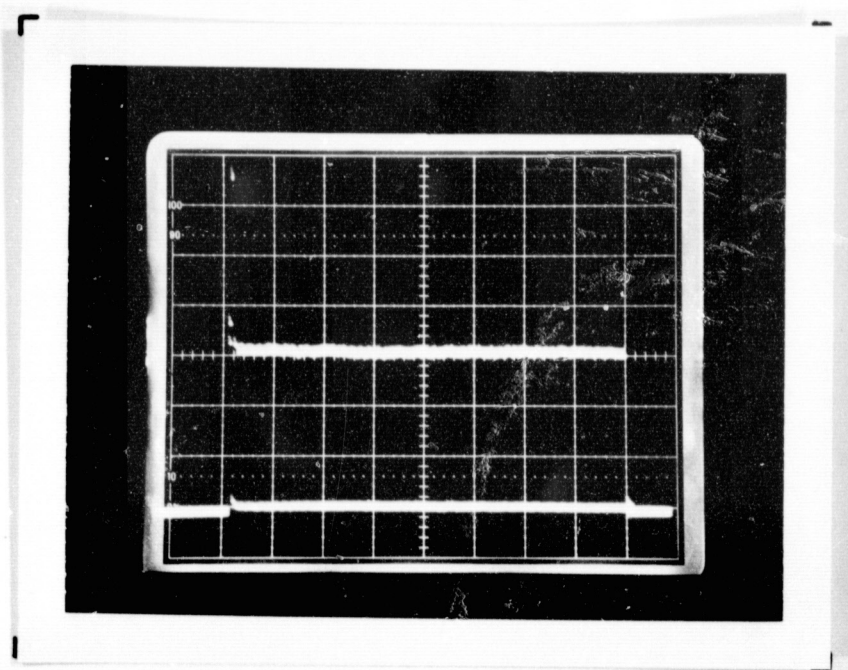
Light source   3400   °K
Spectral filter   0.4000   microns
Average well population   50   %
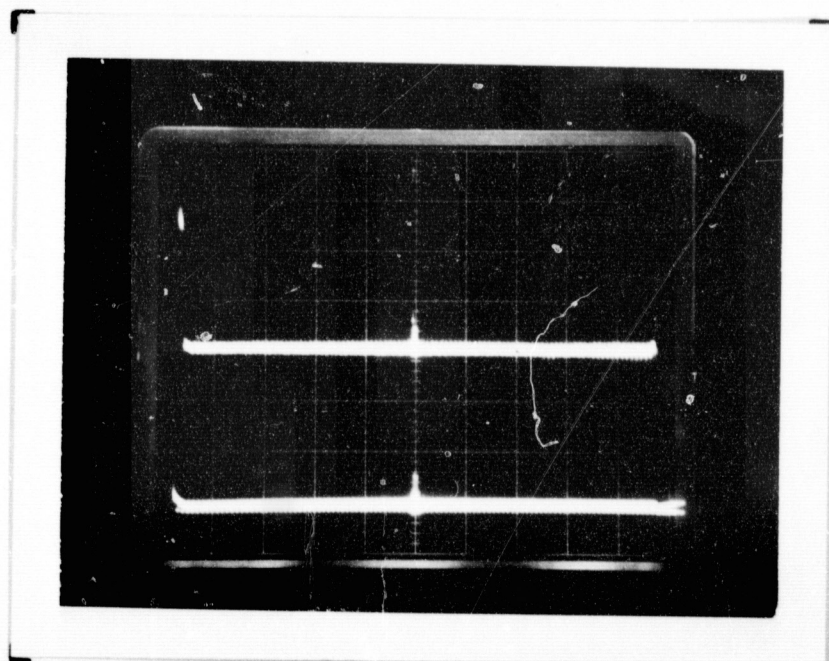Temperature   25   °C
Data rate   1.0   MHz
Frame time   108   ms

81

CCD UNIFORMITY OF RESPONSE

Device Number 284-1-9 Device Type 160 x 100

Light source 3400 °K Spectral filter 0.4000 microns

Average well population 50 % Temperature 25 °C
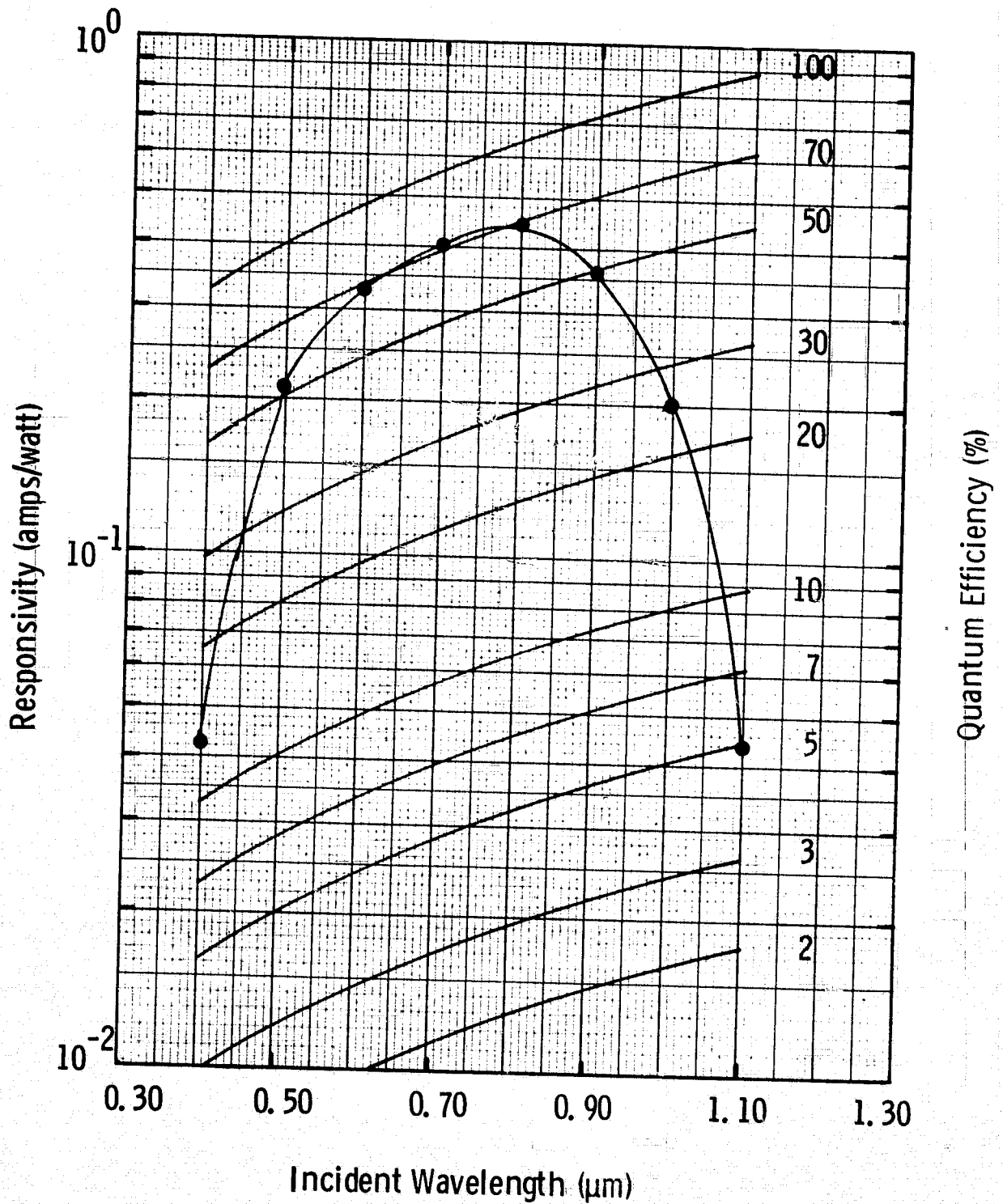
Data rate 1.0 MHz Frame time 108 ms

Oscilloscope presentation
Video line number 50

Oscilloscope presentation
Complete video frame

82

CCD SPECTRAL RESPONSIVITY

Device 284-1-9

Incident Wavelength (μm)

DATA RATE	1.0	MHz
FRAME TIME	32	MS
TEMPERATURE	25	°C

ICCD CHARACTERIZATION REPORT

1. TUBE NUMBER ___278___ DEVICE NUMBER __284-1-9__

2. MANUFACTURER __Varo Electron Devices__

   TUBE TYPE __25 mm electrostatically-focussed triode__

3. TUBE PROCESSING EFFECTS

   Dark Current Changes

	Total (nA)	Active Area Density (nA/cm^2)
Before processing	0.5	3.6
After processing	1.1	10.8

4. PHOTOCATHODE PROPERTIES

   Type __S20__

   Responsivity (See accompanying graphs)

   Broadband (2854 K) __410__ A/lm; 8000 A __3__ mA/W

5. EBS GAIN

   Average EBS gain is __1600__ at __10__ KV; __3300__ at __15__ KV

6. COMMENTS __a dark current bright spot increased into a bright__
   __line during tube processing__
   _____
   _____
   _____

Device Number _Tube#278_   Device Type _160 x 100 Varo Triode_

Light Source _2854_ °K Spectral filter _none_ micros

Temperature _25_ °C Data rate _1.0_ MHz

Frame time _100_ ms Photocathode Illuminance _1.1 x 10^{-4}_ fc

Accelerating Voltage _15_ KV   Focussing Voltage _14.7_ KV